MS-I

PWA FR-986
18 JUNE 1964

RESEARCH AND DEVELOPMENT OF MATERIALS FOR USE AS LUBRICANTS IN A LIQUID HYDROGEN ENVIRONMENT

SUMMARY REPORT

PREPARED UNDER
CONTRACT NAS8-11537
CONTROL NO. 1-3-84-80353 SI(IF)
FOR
PROPULSION AND VEHICLE ENGINEERING LABORATORY
ENGINEERING MATERIALS DIVISION
GEORGE C. MARSHALL SPACE FLIGHT CENTER
HUNTSVILLE, ALABAMA

Pratt & Whitney Aircraft DIVISION OF UNITED AIRCRAFT CORPORATION

FLORIDA RESEARCH & DEVELOPMENT CENTER

4

PWA FR-986
18 JUNE 1964

RESEARCH AND DEVELOPMENT OF MATERIALS FOR USE AS LUBRICANTS IN A LIQUID HYDROGEN ENVIRONMENT

SUMMARY REPORT

Written By:

W. C. Keathley
Program Manager

E. W. Dwyer
Sr. Experimental Engineer

Approved By:

C. R. Comolli
Supervisor

PREPARED UNDER
CONTRACT NAS8-11537
CONTROL NO. 1-3-84-80353 SI(IF)
FOR
PROPULSION AND VEHICLE ENGINEERING LABORATORY
ENGINEERING MATERIALS DIVISION
GEORGE C. MARSHALL SPACE FLIGHT CENTER
HUNTSVILLE, ALABAMA

Pratt & Whitney Aircraft DIVISION OF UNITED AIRCRAFT CORPORATION

FLORIDA RESEARCH & DEVELOPMENT CENTER

FOREWORD

This report was prepared by Pratt & Whitney Aircraft Division of United Aircraft Corporation under Contract NAS8-11537 for the George C. Marshall Space Flight Center of National Aeronautics and Space Administration. The work was administered under the technical direction of the Propulsion and Vehicle Engineering Laboratory, Engineering Materials Division of the George C. Marshall Space Flight Center with Mr. K. E. Demorest acting as Contracting Officers Representative.

CONTENTS

SECTION		PAGE
	ILLUSTRATIONS	iv
	ABSTRACT	vi
I	INTRODUCTION	I-1
II	TEST APPARATUS	II-1
III	SELECTION AND TESTS OF STANDARD MATERIALS	III-1
IV	SELECTION OF CANDIDATE LUBRICANT MATERIALS	IV-1
V	TESTS OF CANDIDATE MATERIALS	V-1

ILLUSTRATIONS

FIGURE		PAGE
II-1	External View of Existing Ball Plate Apparatus........	II-13
II-2	Internal View of Existing Apparatus Showing Retainer and Balls..................................	II-14
II-3	Sketch of Existing Ball Plate Test Apparatus..........	II-15
II-4	Free-Body Diagram of a Ball Operating Under Thrust Load...	II-16
II-5	Free-Body Diagram of a Ball Operating Under Thrust Load at Zero Speed................................	II-17
II-6	Section View Showing Ball Velocity Vectors............	II-18
II-7	Typical Stress-Cycle Curves..........................	II-19
II-8	Relationship of Ball Life to Spin/Roll Ratio..........	II-20
II-9	Hertz Stress vs Thrust Per Ball......................	II-21
II-10	Ratio of Spin Velocity and Roll Velocity vs Thrust Per Ball....................................	II-22
II-11	Ratio of Spin Velocity and Inner Race Velocity vs Thrust Per Ball....................................	II-23
II-12	Hertz Stress vs Thrust Per Ball......................	II-24
II-13	Ratio of Spin Velocity and Roll Velocity vs Thrust Per Ball....................................	II-25
II-14	Ratio of Spin and Inner Race Velocity vs Thrust Per Ball....................................	II-26
II-15	Hertz Stress vs Thrust Per Ball......................	II-27
II-16	Ratio of Spin Velocity and Roll Velocity vs Thrust Per Ball....................................	II-28
II-17	Ratio of Spin Velocity and Inner Race Velocity vs Thrust Per Ball....................................	II-29
II-18	Effect of DN on Ratio of Spin Velocity to Roll Velocity......................................	II-30
II-19	Effect of DN on Ratio of Spin Velocity to Inner Race Velocity......................................	II-31
II-20	Angular and Vectorial Relationships for Ball Plate Test Apparatus................................	II-32
II-21	Ball-Plate Test Apparatus............................	II-33
II-22	Overall View of Ball Plate Test Apparatus.............	II-34
II-23	Closeup of Ball Plate Test Apparatus	II-35
III-1	Summary of Bearing Lubricant Test Results............	III-6
III-2	View of Wear Path in Outer "V" Showing Most Severe Pitting Present on Part. (Test No. 3, Rulon A at DN = 4 x 10^6 mm-rpm)................................	III-7
III-3	View of Typical Spalls in Wear Path. Photos were Taken from Chromium Shadowed Replicas (Test No. 3, Rulon A at DN = 4 x 10^6 mm-rpm)......................	III-8
III-4	View of Circumferential Section Through the Inner Wear Path of the Outer "V" Showing Typical Spalls. AISI 440C Material (Test No. 3, Rulon A at DN = 4 x 10^6 mm-rpm)................................	III-9

ILLUSTRATIONS
(Continued)

FIGURE		PAGE
III-5	Typical Surface Spalling (Rulon A after 2.6 Hours at DN = 4×10^6, Mag = 30x)	III-10
III-6	Typical Unshrouded Insert Wear	III-11
III-7	Typical Shrouded Insert Wear	III-12
V-1	Typical Retainer Insert Wear (Ag-Mo S_2 After 10 Hours at Equivalent DN Value of 4×10^6 mm-rpm)	V-13
V-2	Typical Retainer Insert Wear (Ag-Ca F_2 After 3.5 Hours at Equivalent DN Value of 2×10^6 mm-rpm)	V-14
V-3	Salox M Insert Wear	V-15
V-4	Typical Retainer Insert Wear (BN After 5.5 Hours at Equivalent DN Value of 2×10^6 mm-rpm)	V-16
V-5	Typical Retainer Insert Wear (SP-3 After 10 Hours at Equivalent DN Value of 2×10^6 mm-rpm)	V-17
V-6	Typical Retainer Insert Wear (Salox Z-1 After 10 Hours at Equivalent DN Value of 2×10^6 mm-rpm)	V-18
V-7	Al-MoS_2 Insert After 10 Hours Operation at DN = 2×10^6 mm-rpm	V-19

ABSTRACT

27311

A program was conducted to evaluate materials which could be used as lubricants in anti-friction bearings operating in a liquid hydrogen environment at DN values from 2×10^6 to 4×10^6 mm-rpm. Even though no tests were conducted in a nuclear radiation field, consideration was given to such an environment in the selection of some of the candidate materials. The program described herein resulted in the discovery of a material which provides a significant increase in the possible bearing life when operating under the above conditions.

Author:

SECTION I
INTRODUCTION

The technical mission of this program is two-fold: (1) Develop, test and evaluate lubricating methods for bearings operating in liquid hydrogen at equivalent DN values from 2×10^6 to 4×10^6 mm-rpm (DN value is the product of bearing bore in millimeters and shaft speed in revolutions per minute) and (2) develop data of design significance which illustrate the relationship of bearing performance (such as rotational speed and load) for specific lubricating methods employed on bearings operating in liquid hydrogen at equivalent DN values from 2×10^6 to 4×10^6 mm-rpm.

These goals were pursued in four separate but inter-related work tasks. They were:

1. Development of Test Apparatus

This work task included the modification and testing of an existing test apparatus for the simulation of conditions compatible with ball bearing environments that exist in liquid hydrogen rocket engine turbomachinery. The test apparatus was required to evaluate lubricants at equivalent DN values of 2×10^6 to 4×10^6 mm-rpm while the test specimens were completely submerged in liquid hydrogen and subjected to Hertzian stresses encountered in actual turbopump bearings.

2. Selection and Tests of Standard Lubricant Materials

The purpose of this task was to select a lubricant which is presently employed in a liquid hydrogen application and conduct baseline tests with this lubricant, the results of which can be used for comparison to the results of subsequent candidate materials tests.

3. Selection of Candidate Lubricants

Concurrently with the modification of the test apparatus, a literature search was conducted to gather information on lubricants and lubricating systems which would most likely be successful when subjected to the specified test conditions. Consideration was also given throughout the study to materials having resistance to nuclear radiation.

4. Experimental Evaluation of Candidate Lubricant

This task included tests of the selected candidate materials. Each specimen was subjected to two tests at an equivalent DN value of 2×10^6 mm-rpm and to the same environment and loads used in the standard material in the low DN tests. If the material's performance was comparable to the standard material at the low DN tests, the candidate would then be tested at a higher DN value.

The results of this program have shown that ball bearings using AISI 440C balls and plates and Salox M (bronze-filled polytetra fluorethylene) retainers could be expected to operate satisfactorily for more than 10 hours in liquid hydrogen at DN values up to 4×10^6 mm-rpm. It is interesting to note that recent experience gained with an RL10 engine bearing strengthens this conclusion where a 35-millimeter ball bearing, using Salox M retainers, has been tested under the following conditions.

Speed	Load		Time
30,000	600 lb thrust		12 hours
12,000	150 lb thrust 500 lb radial		75 hours
		Total Time	87 hours

Inspection of the bearing after the above test schedule showed the bearing to be in excellent condition and the bearing has been reinstalled in the test apparatus for further endurance running. It should be pointed out that the Hertzian stresses in the above test conditions are approximately 180,000 psi and the spin/roll ratios are approximately .15, which are not as strict as the test conditions imposed on the candidate materials used in the experimental phases of this program.

SECTION II
TEST APPARATUS

Almost everyone subscribes to the fact that a true evaluation of a bearing lubricant cannot be achieved by testing actual bearings. There are many interactions associated with an operating bearing which can affect the life of the bearing but which have nothing whatsoever to do with the lubrication process. A simple example involves the structural problems with a rotating retainer. Of course, lubricants developed and evaluated in simulating devices should, in the final stage, be tested in actual ball bearings; but the test apparatus used to initially select the most effective lubricants should eliminate as many extraneous effects as possible.

An existing test apparatus, which has been used in similar programs at Pratt & Whitney Aircraft over the past several years, was modified to permit cryogenic testing and utilized in this test program. It was specifically designed to simulate various levels of Hertzian stress (contact stress), slip in the contact zone, and ball rotational velocity in a retainer pocket. In simulating the above parameters, this test apparatus is designed consistent with a theory of failure that in general terms states the principal causes of surface fatigue to be (1) level of Hertzian stress in the contact zone and (2) slip in the contact zone. The slip in the contact zone causes surface damage which reduces the fatigue strength of the material and therefore reduces the life of the surface for a given level of contact stress. The purpose of the lubricant is therefore to reduce the amount of surface damage caused by the slip in the contact zone. The optimum lubricant would, of course, eliminate the damage completely and the surface would fail at a life equal to its pure rolling contact endurance life. This theory of failure is described more fully in a later section of this report.

The existing ball-plate test apparatus, as shown in figure II-1 and II-2, was developed several years ago to determine specific bearing operating limitations related to lubricants and bearing steels. In general, this unit eliminates the use of test bearings in the initial screening phase where the important factor is to evaluate lubricants and other bearing materials without the confounding effect of extraneous bearing parameters. In addition to providing a more accurate evaluation of a lubricant, it also eliminates the cost of special test bearings and appreciably reduces the parts procurement time. This test apparatus can be considered as a fundamental evaluation tool making possible a test technique akin to tensile testing of metals, whereby material properties are evaluated prior to fabrication of an operational part.

A sketch of the existing ball-plate test apparatus is shown in figure II-3. The two test plates and balls are located in a separate housing in the center of the assembly.

On either side of the center housing, the shafts that carry the test plates are supported by oil-lubricated rolling element bearings. The test plates are counter-rotating and are each driven by an electric motor. The bearing load is applied by placing dead weights on the end of the lever arm, which is attached to the left shaft support assembly. This assembly is free to slide axially; thereby transmitting thrust directly to the rotating plate. An expanded view of the test plates, balls and retainers is also shown in figure II-3.

Since the plates rotate in the opposite direction at approximately the same speed, the retainer rotates very slowly and serves only to prevent the balls from changing their angular orientation. This arrangement also means that relatively low speed drives can be used to obtain tests at high equivalent DN values.

Fatigue failures are indicated by an accelerometer, which is located on the loading lever and indicates acceleration in the axial direction. This technique has proved highly successful and small changes in the surface of a ball or race are easily detected. The millivolt output of the accelerometer is fed into an automatic abort system and shuts off the drive power when the output reaches a predetermined value.

Referring to figure II-3, the ball rotation about its own axis is a function of the groove diameter and the speeds of the shafts. To obtain different ball speeds at constant shaft speeds, one has only to place the ball in any one of the two concentric grooves in the plate.

The Hertzian stress level can be adjusted by changing the included angle of the groove and/or the applied axial loads. For a constant applied dead weight on the lever arm, the Hertzian stress to which the ball and grooved plate are subjected is a function of the ball diameter and the groove angle.

Ball spin will occur about an axis drawn from the grooved plate contact points and the ball center and is controlled by varying the plate groove angle.

The test plates, retainer, and balls can be changed and inspected by separating the center housing of the bearing test cavity. This is an economical feature because the assembly time and test set-up time can be minimized. The test apparatus can remain on the test stand throughout the experimental program, thus reducing the man hours associated with mounting, instrumentation hookup, etc.

As stated before, the contract requires that the standard and candidate lubricants be tested at conditions that would exist in a rocket engine ball bearing operating in liquid hydrogen at DN values of 2×10^6 and 4×10^6 mm-rpm. Since fatigue damage to ball bearings occurs as a result of the Hertzian stress level and the amount of spin in the ball-race contact area, an analysis was conducted to determine the Hertzian stress and spin that exist in typical rocket engine ball bearings operating at the specified DN levels.

Before proceeding to the methods used in this analysis it is appropriate to review basic ball bearing dynamics and various terms which will be used throughout this discussion.

Figure II-4 shows a free-body diagram of a ball operating under a thrust load of T/n (n is the number of balls in the pitch circle and T is the total bearing thrust load) at some rotational speed.

Figure II-5 shows the same ball operating under the same thrust load but at zero speed. Note that the outer race contact angle, βo, of the rotating ball is smaller than the static contact angle, and that the inner race contact angle, βi, becomes greater with rotation.

The ball has two axes of rotation, (1) about the bearing centerline and (2) about the ball roll axis, A-A. There is a third possible axis (B-B) of rotation as shown in figure II-4; however, absolute ball rotation about this axis is not evident from a review of high-speed motion pictures of ball bearing tests. This fact indicates that there is relative slip between the ball and inner race contact zone. This phenomenon can be seen using the vector triangle in figure II-6.

If A-A is the axis of rotation for the ball, vector $\bar{\omega}_B$ represents the absolute ball rotational velocity of the ball, and vector $\bar{\omega}_R$ represents the relative rolling velocity of the ball relative to the inner race. To close the triangle a vector $\bar{\omega}_S$ must exist, and is customarily called the relative spin (slip) vector.

Also shown in figure II-6 is an enlarged view of the inner race contact zone. It can be seen that the upper edge of the contact zone is traveling slower than the lower edge ($r_1 \cdot \omega_B < r_2 \cdot \omega_B$); thus, there will be a tendency toward ball spin in the contact zone.

Excluding the possibility of a retainer failure, a ball bearing will fail when a spot on the surface of one of its elements (ball, inner race, or outer race) ruptures from fatigue due to a vibratory stress. (The steady or constant stresses on these elements are insignificant.) The number of cycles which a material can withstand at various vibratory stress levels is usually depicted by a S-N (vibration stress level - life in cycles) curve similar to the solid line shown in figure II-7. If the material is subjected to a vibratory stress level, σ_1, then it will last 10^7 stress cycles and more. This value of 10^7 cycles is referred to as the runout life, meaning that if a stressed material lasts 10^7 cycles, it will not fail, no matter how many additional cycles are imposed. This is certainly not rigidly true but is sufficiently accurate for this discussion. If the material is stressed to σ_2, the material will fail at 10^n cycles where $n<7$. This curve is generally used in showing the fatigue strength of beams and other structural members when subjected to vibratory bending (tensile, and compressive) loads. However, the same effect is true with respect to a surface under contact compression; the only difference being that the surface does not experience complete stress reversals. The cycle goes from zero stress to maximum compressive stress and back to zero stress.

The dotted line on figure II-7 shows the effect of surface notching on fatigue life. The notching effect in ball bearings results from surface fretting where spinning or slipping occurs in the contact zones. Under such conditions of contact zone slip, the material surface is damaged and the fatigue life of the material is reduced for any given stress level. So as surface slip occurs, and surface damage accumulates, the S-N curve shifts downward with increasing number of cycles. After the surface damage has evolved, the life for instance, would be 10^m at a stress level of σ_1 instead of the runout life that would be available with no slip (no surface damage). In actual application figure II-8 shows experimental data for the effect of life of an oil-lubricated ball subjected to a constant Hertzian stress and various ratios of spin velocity to roll velocity. For a cryogenic bearing application, the curve would move appreciably to the left because of the higher coefficient of friction and correspondingly greater surface damage at any given level of slip. This curve confirms the important effect of contact zone slip on life and generally speaking, substantiates the conclusion that the prime factors governing the life of a bearing are the slip in the contact zone and the Hertzian stress.

It is now clear that for a true evaluation of a lubricant, Hertzian stress in the contact zone, spin/roll velocity ratios, and ball rotational velocity must be defined and simulated in the test apparatus. To determine the required level of these parameters, Pratt & Whitney Aircraft utilized an existing mathematical model which predicts the ball bearing internal dynamics for any combination of speed and thrust load. A set of three curves were produced for each of three bearing designs. The size of these bearings (bore diameters of 40, 60, and 80 millimeters) were chosen for compatibility with requirements indicated in many preliminary studies of advanced liquid rocket hydrogen/oxygen engines. These studies have been conducted by Pratt & Whitney Aircraft over the past three years. The internal geometries which were selected for each bearing size are based on many years of theoretical and experimental studies which Pratt & Whitney has conducted with cryogenically-cooled ball bearings.

The three sets of curves shown in figures II-9 through II-17 were produced for each bearing design and represented the following relationships:

a. The effect of thrust per ball on the inner and outer race Hertzian stresses for DN values of 2×10^6, 3×10^6, and 4×10^6 mm-rpm.

b. The effect of thrust per ball on the ratio of spin velocity to roll velocity for DN values of 2×10^6, 3×10^6, and 4×10^6 mm-rpm.

c. The effect of thrust per ball on the ratio of spin velocity to inner race velocity for DN values of 2×10^6, 3×10^6, and 4×10^6 mm-rpm.

Using these relationships, one can enter a stress curve for a given bearing at a specific Hertzian stress level and read the thrust per ball that would exist for the appropriate speed. In this program an inner race Hertzian stress of 250,000 psi was chosen since this level is considered near the maximum value permissible for reliable bearing design.

With the thrust per ball determined from the stress curve the spin/roll and spin/inner race velocity curves can be entered at the appropriate thrust per ball and the required velocity ratios can be determined.

The results of this method of analysis can be summarized on plots shown in figures II-18 and II-19 where the spin/roll velocity ratio and spin/inner race velocity ratio is shown as a function of bearing DN value for a constant inner race Hertzian stress level of 250,000 psi. Since the program specifies tests at equivalent DN values of 2×10^6 and 4×10^6 mm-rpm, the required velocity ratios are thereby established for these DN values assuming an inner race Hertzian stress of 250,000 psi. These test conditions are indicated on the summary curves, and given in table II-1.

Table II-1. Program Test Conditions

DN values	2×10^6 mm-rpm	4×10^6 mm-rpm
Hertzian stress	250,000 psi	250,000 psi
Spin/roll velocity ratio	.168	.295
Spin/inner race velocity ratio	.72	1.25

Since the above specific Hertzian stress level, amount of spin in the ball-race contact zone that occurs in actual ball bearings and ball rotational velocity must be simulated in the ball-plate test apparatus to be used in this program, a second study was conducted to determine the required rig speed, ball diameter, included angle of the grooved ball track, and the radius of the grooved ball track. A summary of the results is presented in table II-2.

Table II-2. Test Apparatus Parameters

Rpm	10,000	10,000
DN, mm-rpm	2×10^6	4×10^6
R_{rig}, in.	2.03	4.0
α, degrees	9.54	16.5
cos α	0.986	0.958
ω_B, rpm	109,000	221,000
d, in.	0.378	0.378
Total Thrust, lb	214.5	208.5
Plate Groove Angle (θ), degrees	161	147

The following calculations were used to obtain this information:

For constant applied thrust load on the rig, the Hertz stress to which the ball and grooved plate are subjected is a function of the ball diameter and the groove angle. See figure II-20 for appropriate angular and vectoral relationships. The final configuration of the ball-plate apparatus is calculated from the following equations:

$$\frac{\omega_s}{\omega_r} = \tan \alpha$$

Ratio of ball slip to ball roll equals the tangent of the contact angle (α)

$$\omega_{rig} = \frac{\omega_B\, r \cos \alpha}{R_{rig}}$$

Rig speed, grooved plate see figure II-20(A)

$$\omega_B = \frac{\omega_r}{\cos \alpha}$$

Ball Speed
See figure II-20(B).

$$\sigma_m = \frac{N_L}{\pi a^2}$$

Mean Hertzian contact stress

$$a = 0.881 \left(\frac{N_L d}{E} \right)^{1/3}$$

Contact circle radius

$$P = 2N_L \cos \alpha$$

Thrust load
See figure II-20(C).

2. Ball-Race Configuration for DN = 4×10^6 mm rpm

$$\alpha = \tan^{-1} \times 0.295 = 16.5° \qquad \cos \alpha = 0.958$$

Ball Speed

$$\omega_B = \frac{\omega_r}{\cos \alpha} = \frac{\omega_s}{0.295 \cos \alpha} = \frac{1.25\ \Omega}{0.295 \cos \alpha}$$

$$= \frac{1.25 \times 50{,}000}{0.295 \times 0.958} = 221{,}000 \text{ rpm}$$

Ball Diameter (R_{rig} = 4 inches)

$$\omega_{rig} = \omega_B\ r \cos \alpha / R_{rig}$$

$$r = \frac{\omega_{rig} R_{rig}}{\omega_B \cos \alpha} = \frac{10{,}000 \times 4}{221{,}000 \times 0.958} = 0.189 \text{ inch}$$

$d = 0.378$ inch: Use std 3/8 in. dia ball

3. Ball-Race Configuration for DN = 2×10^6 mm rpm

$$\alpha = \tan^{-1} \times 0.168 = 9.54° \qquad \cos \alpha = 0.986$$

Ball Speed

$$\omega_B = \frac{\omega_r}{\cos \alpha} = \frac{\omega_s}{0.168 \cos \alpha} = \frac{0.72\ \Omega}{0.168 \cos \alpha}$$

$$= \frac{0.72 \times 25{,}000}{0.168 \times 0.983} = 109{,}000 \text{ rpm}$$

Radius to Ball Race

$$R_{rig} = \frac{\omega_B \ r \ \cos \alpha}{\omega_{rig}} = \frac{109{,}000 \times 0.189 \times 0.986}{10{,}000} = 2.03 \text{ inch}$$

Thrust Load on Rig

$$\sigma_m = \frac{N_L}{\pi a^2} \qquad\qquad a = 0.881 \left(\frac{N_L d}{E}\right)^{1/3}$$

$$N_L^{1/3} = \frac{\sigma m \ \pi \ (0.881)^2 N_L^{2/3} \ d^{2/3}}{E^{2/3}} = \frac{250{,}000 \ \pi (0.776)(0.378)^{2/3}}{30^{2/3} \times (10^6)^{2/3}}$$

$$= 3.31$$

$$N_L = (3.31)^3 = \underline{\underline{36.3 \text{ lb}}}$$

$$P_{DN2} = 2N_L \cos \alpha = 72.6 \times 0.986 = 71.5 \text{ lb}$$

Total Thrust (3 balls) = 214.5 lb

$$P_{DN4} = 2N_L \cos \alpha = 72.6 \times 0.958 = 69.5 \text{ lb}$$

Total Thrust (3 balls) = 208.5 lb

SYMBOLS

SYMBOL	UNITS	DESCRIPTION
a	Inches	Radius of contact circle
d	Inches	Ball diameter
r	Inches	Radius of ball
D	Millimeters	Bearing base diameter
DN	mm x rpm	Bearing bore diameter in millimeters times shaft speed in rpm
E	psi	Modulus of Elasticity
N	Rev/Min	RPM
N_L	Pounds	Normal load at ball contact
P	Pounds	Thrust load per ball
P_{DN2}	Pounds	Thrust load per ball for simulated 2×10^6 DN operation
P_{DN4}	Pounds	Thrust load per ball for simulated 4×10^6 DN operation
R_{rig}	Inches	Radius from rig centerline to groove in ball race way
α	Degrees	Angle measured from bottom of V groove to point of ball contact
σ_m	psi	Mean Hertzian contact stress
ω_B	Rev/Min	Ball rotational velocity
ω_r	Rev/Min	Spin component of ball rotational velocity
ω_{rig}	Rev/Min	Rig rotational velocity
ω_s	Rev/Min	Roll component of ball rotational velocity
Ω	Rev/Min	Race rotational velocity

Before the existing test apparatus, which was discussed above, could be used in this program certain modifications were necessary to permit testing with a cryogenic fluid. These modifications included:

1. Increasing the test plate diameter in the test compartment.
2. Increasing the diameter of the intermediate housing that surrounds the larger test plates.
3. Installing twin seals at both ends of the test compartment to prevent any mixing of the hydrogen in the test compartment and the oil in the adjacent bearing compartments.

A sketch of the modified test apparatus is shown in figure II-21. Photographs of various views of the actual rig are shown in figures II-22, and II-23.

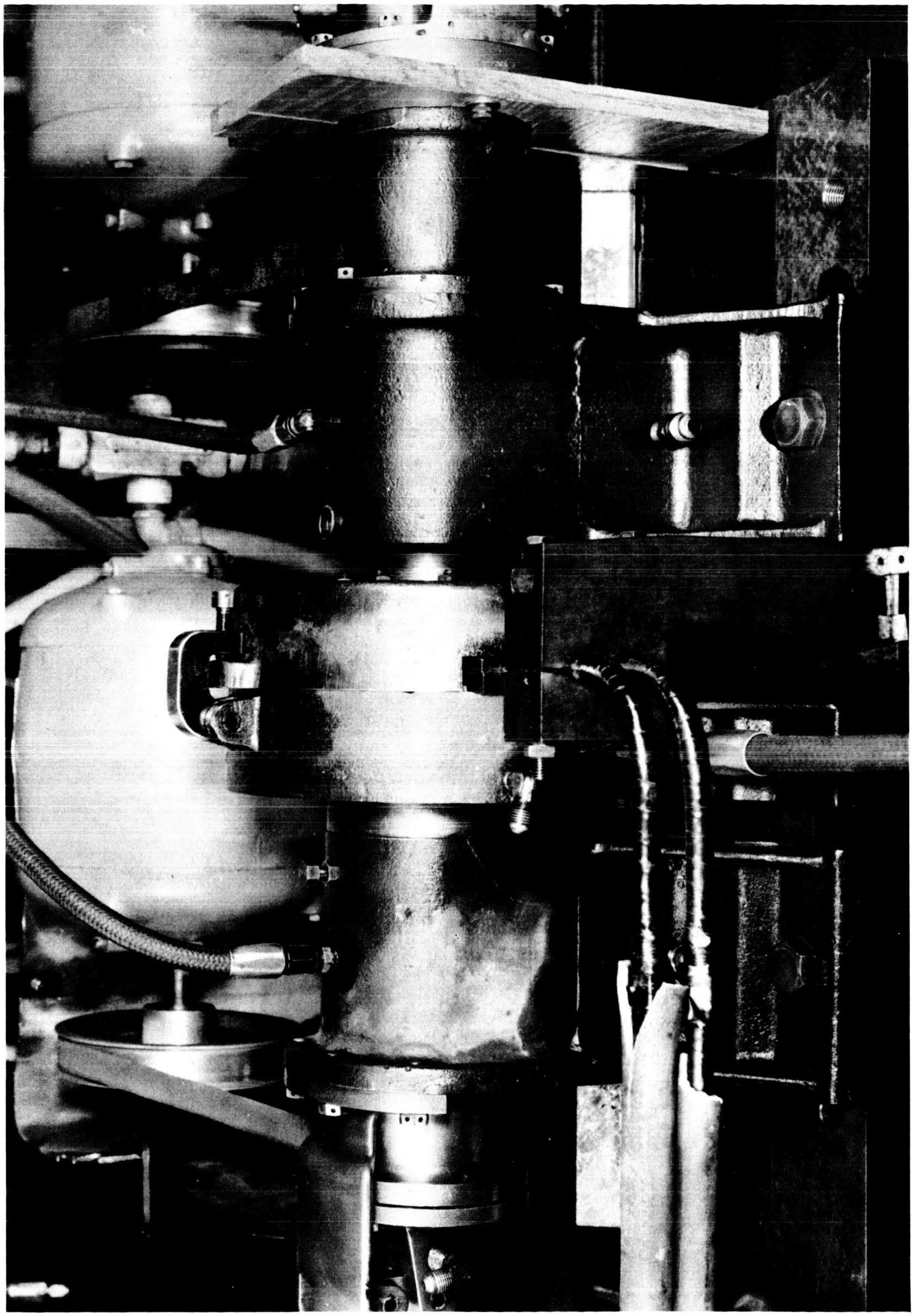

FD 5638

Figure II-1. External View of Existing Ball Plate Apparatus

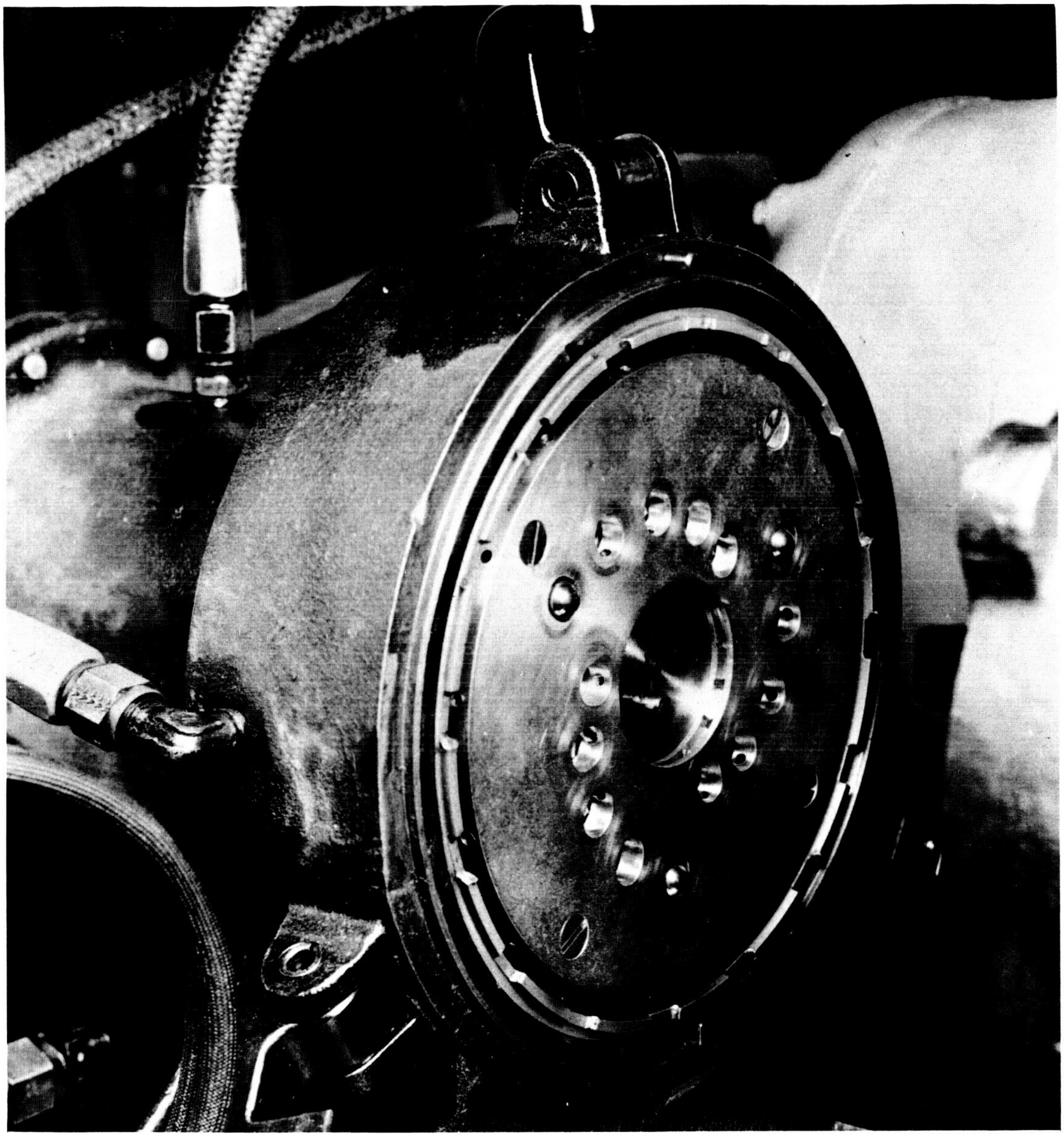

Figure II-2. Internal View of Existing Apparatus Showing Retainer and Balls FD 5637

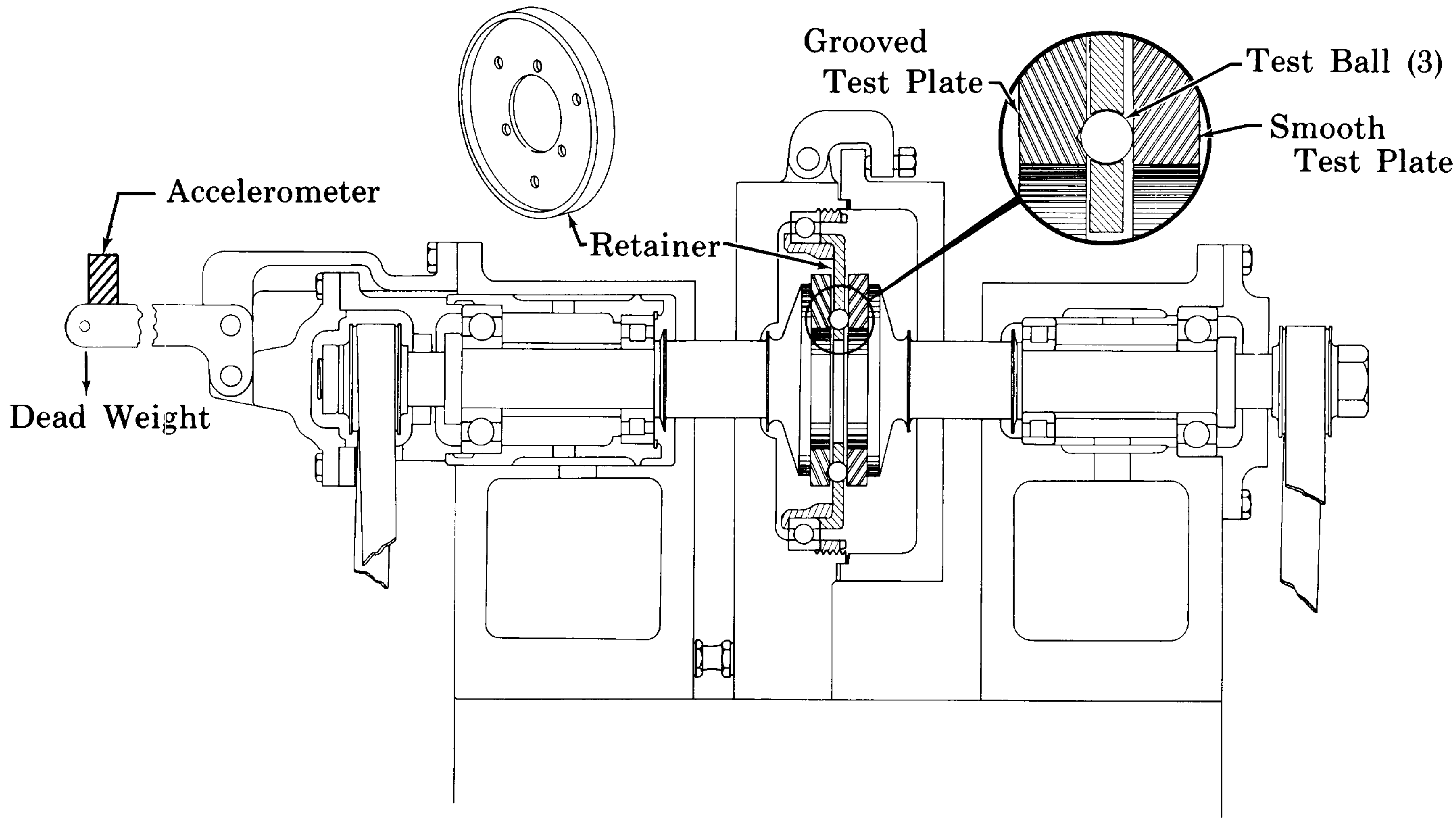

Figure II-3. Sketch of Existing Ball-Plate Test Apparatus

FD 5641A

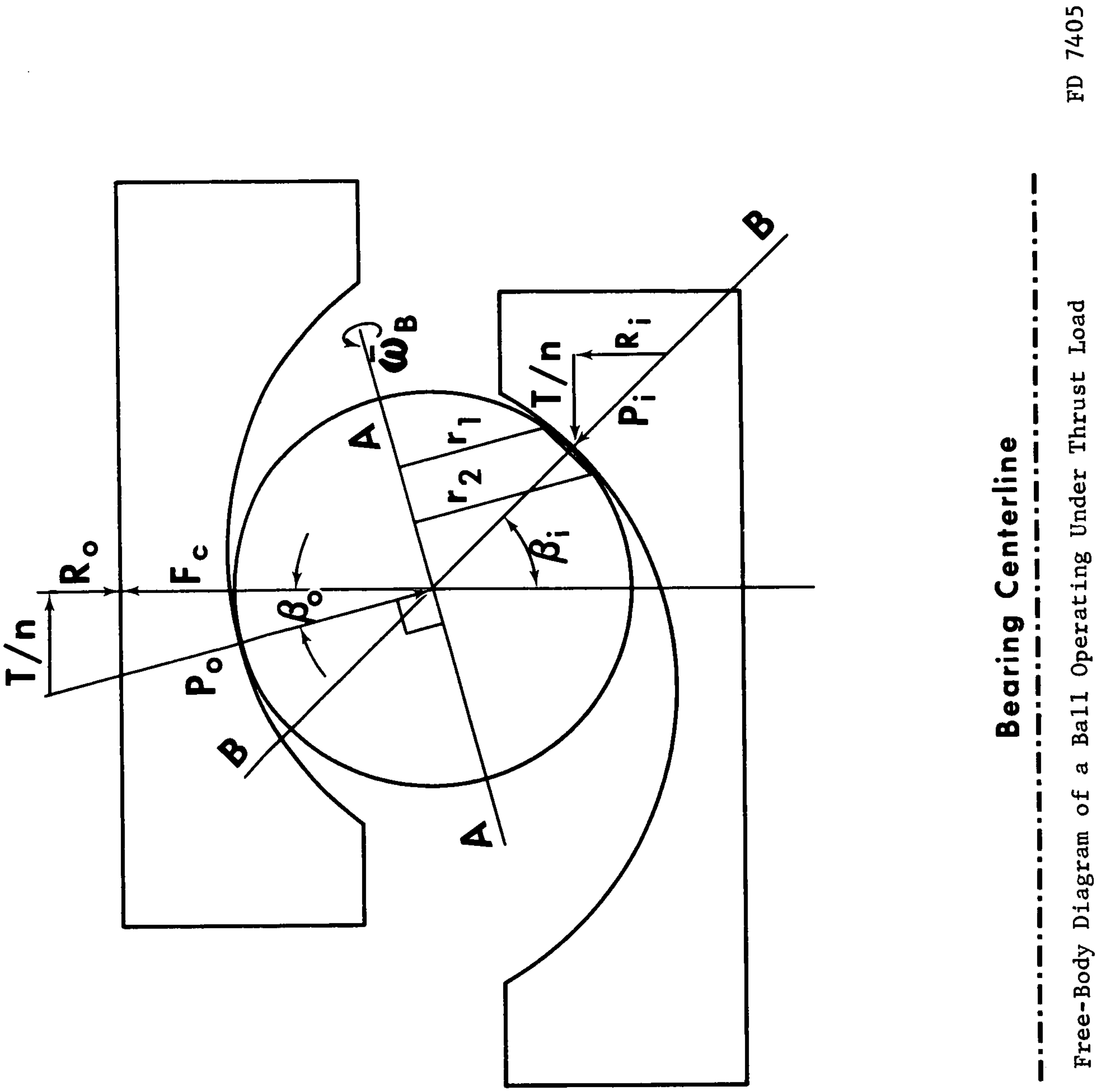

Figure II-4. Free-Body Diagram of a Ball Operating Under Thrust Load

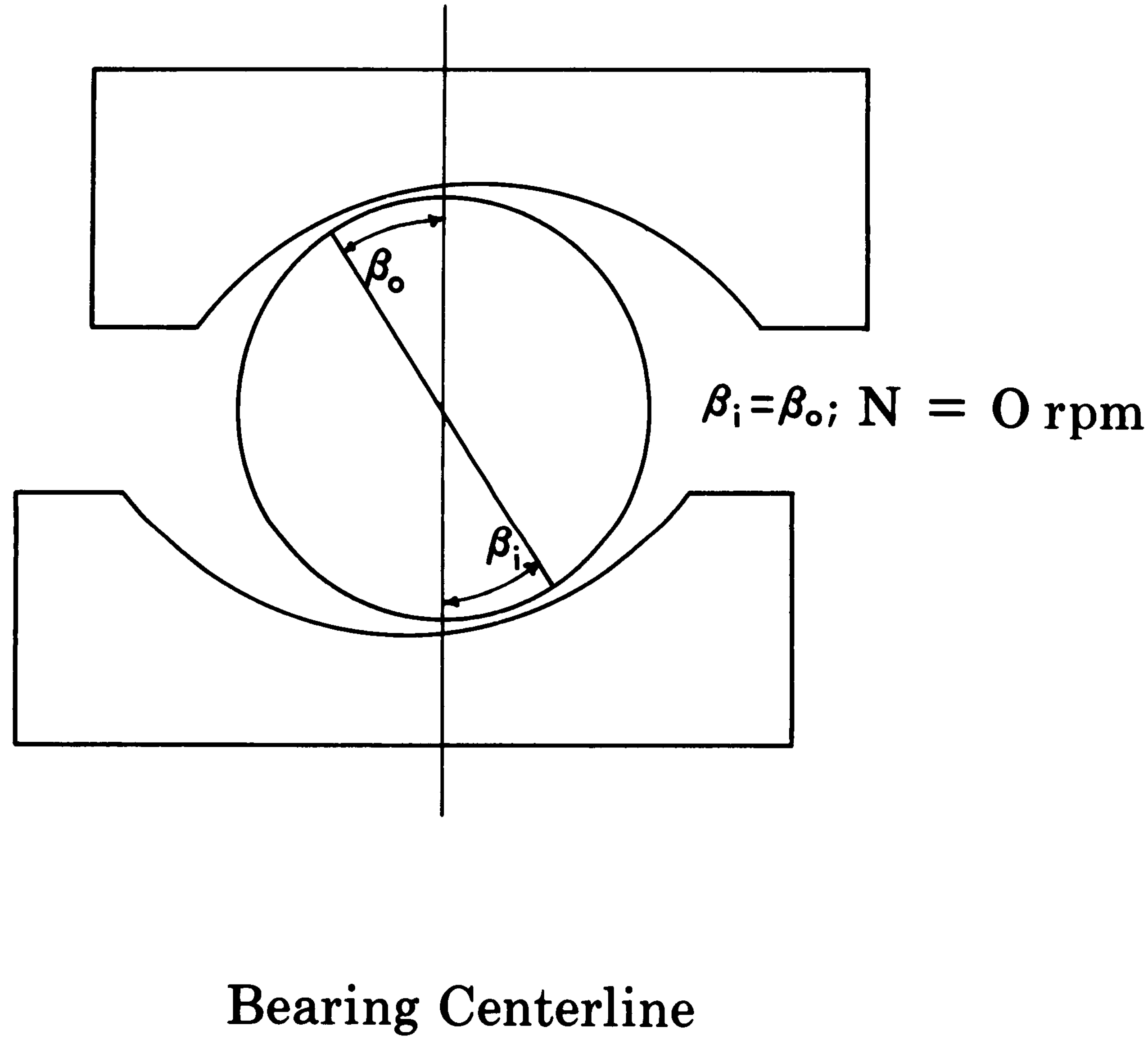

Figure II-5. Free-Body Diagram of a Ball Operating Under Thrust Load at Zero Speed

FD 7406A

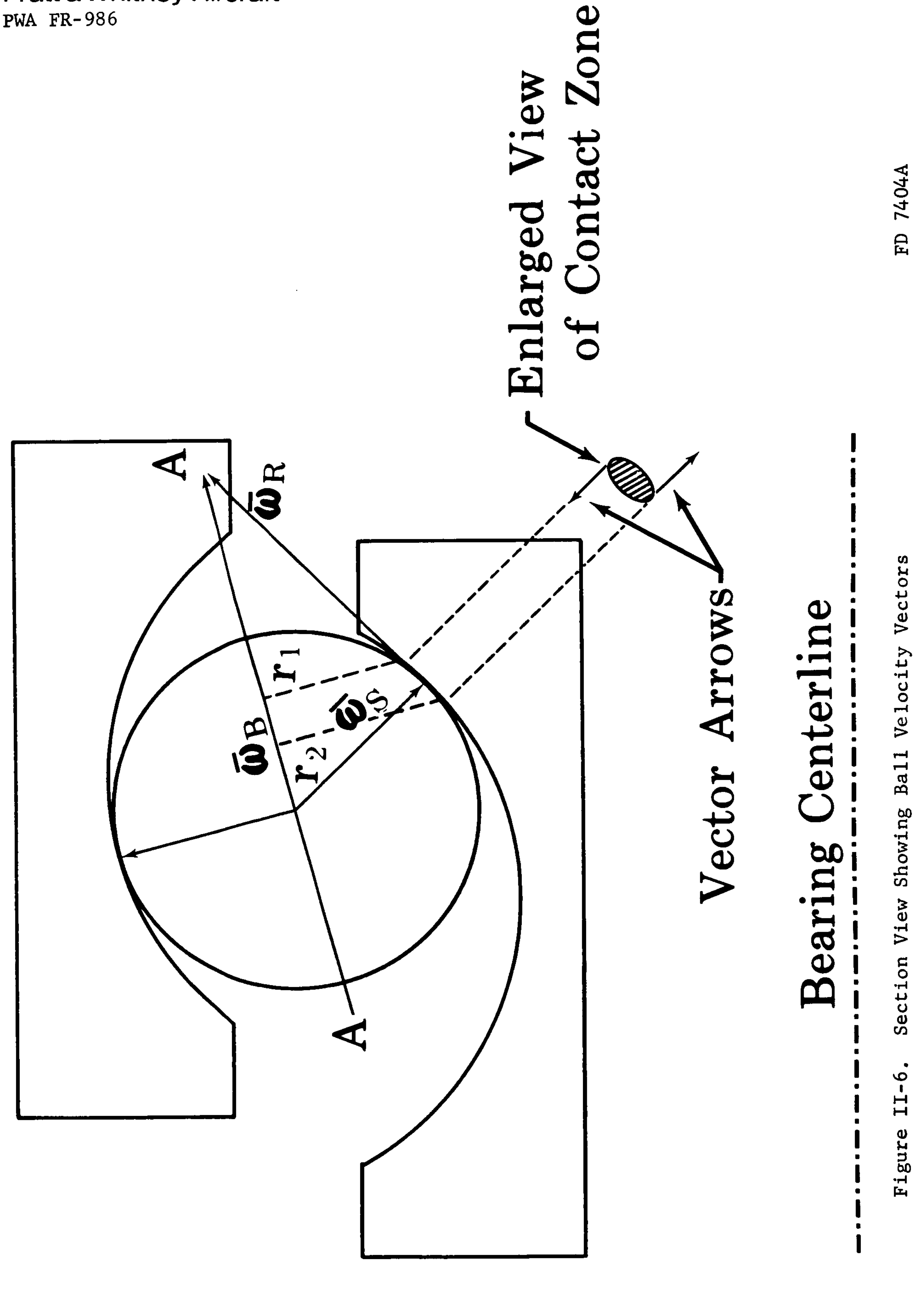

Figure II-6. Section View Showing Ball Velocity Vectors

FD 7359A

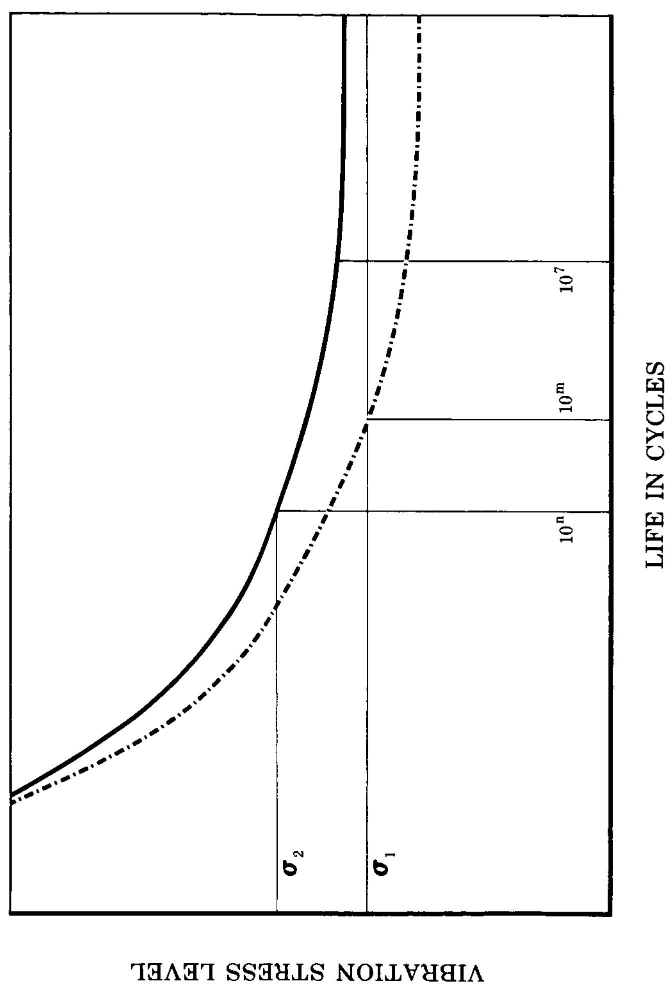

Figure II-7. Typical Stress-Cycle Curves

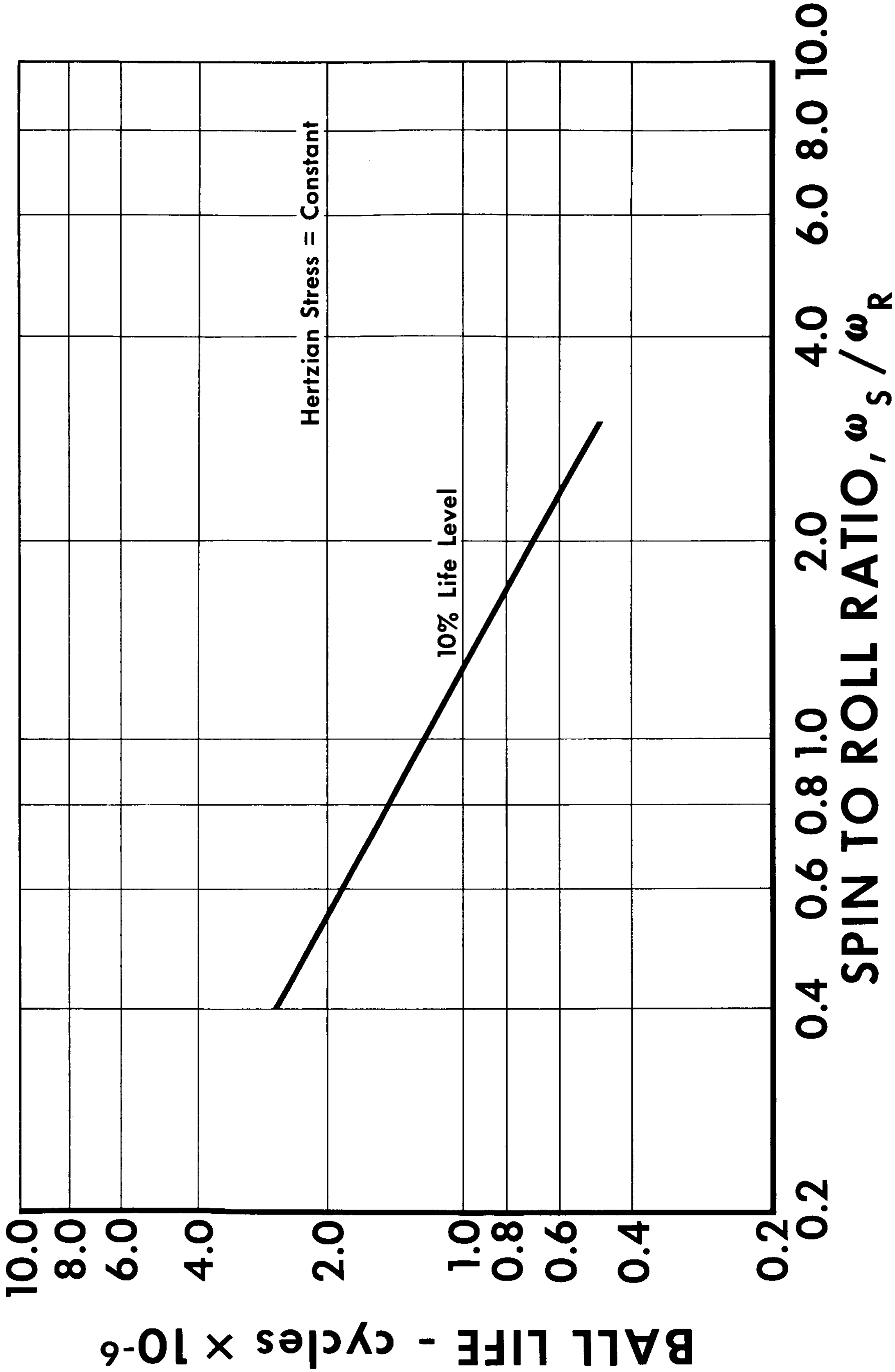

FD 7358

Figure II-8. Relationship of Ball Life to Spin/Roll Ratio

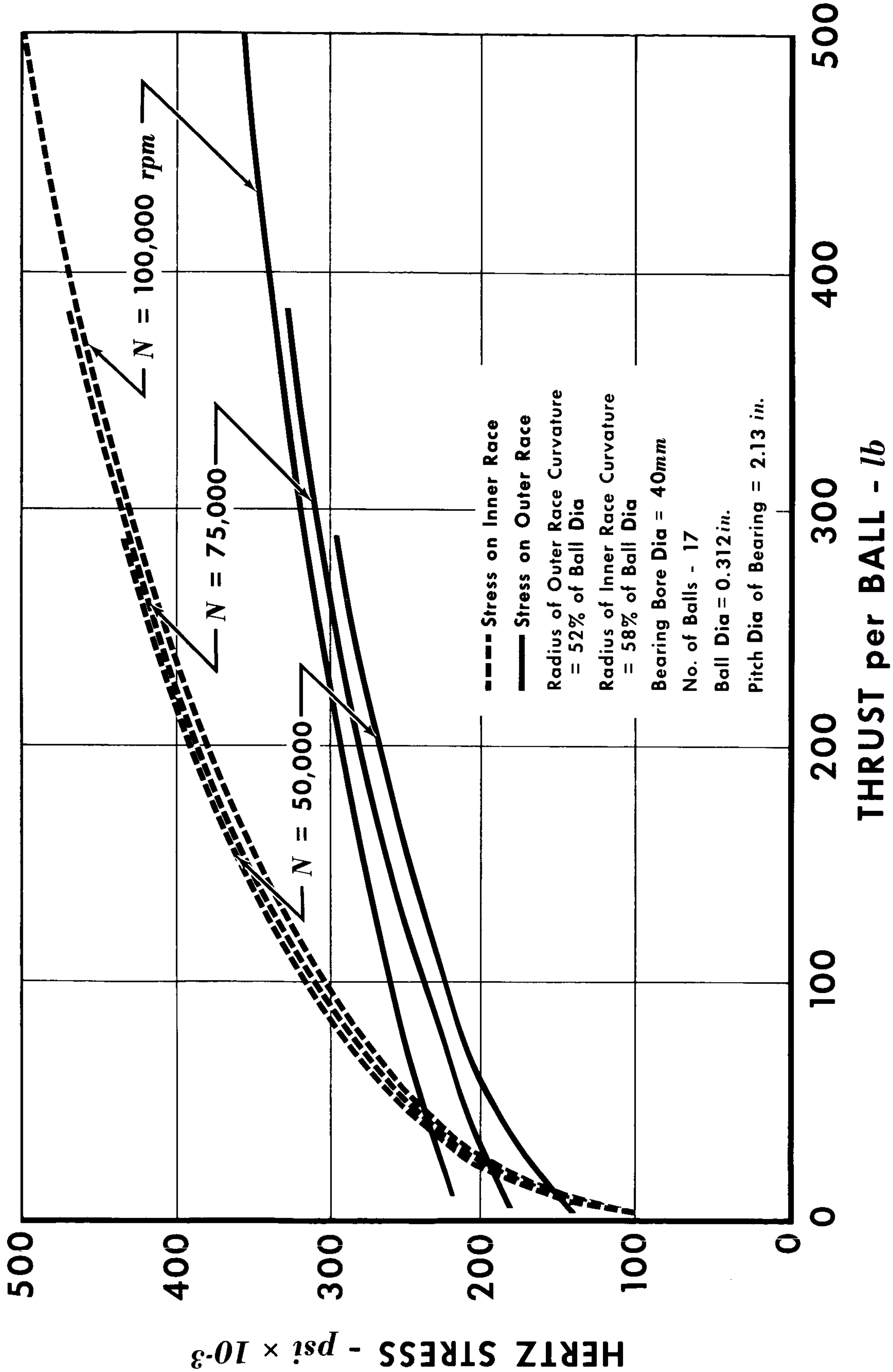

FD 6730

Figure II-9. Hertz Stress vs Thrust Per Ball

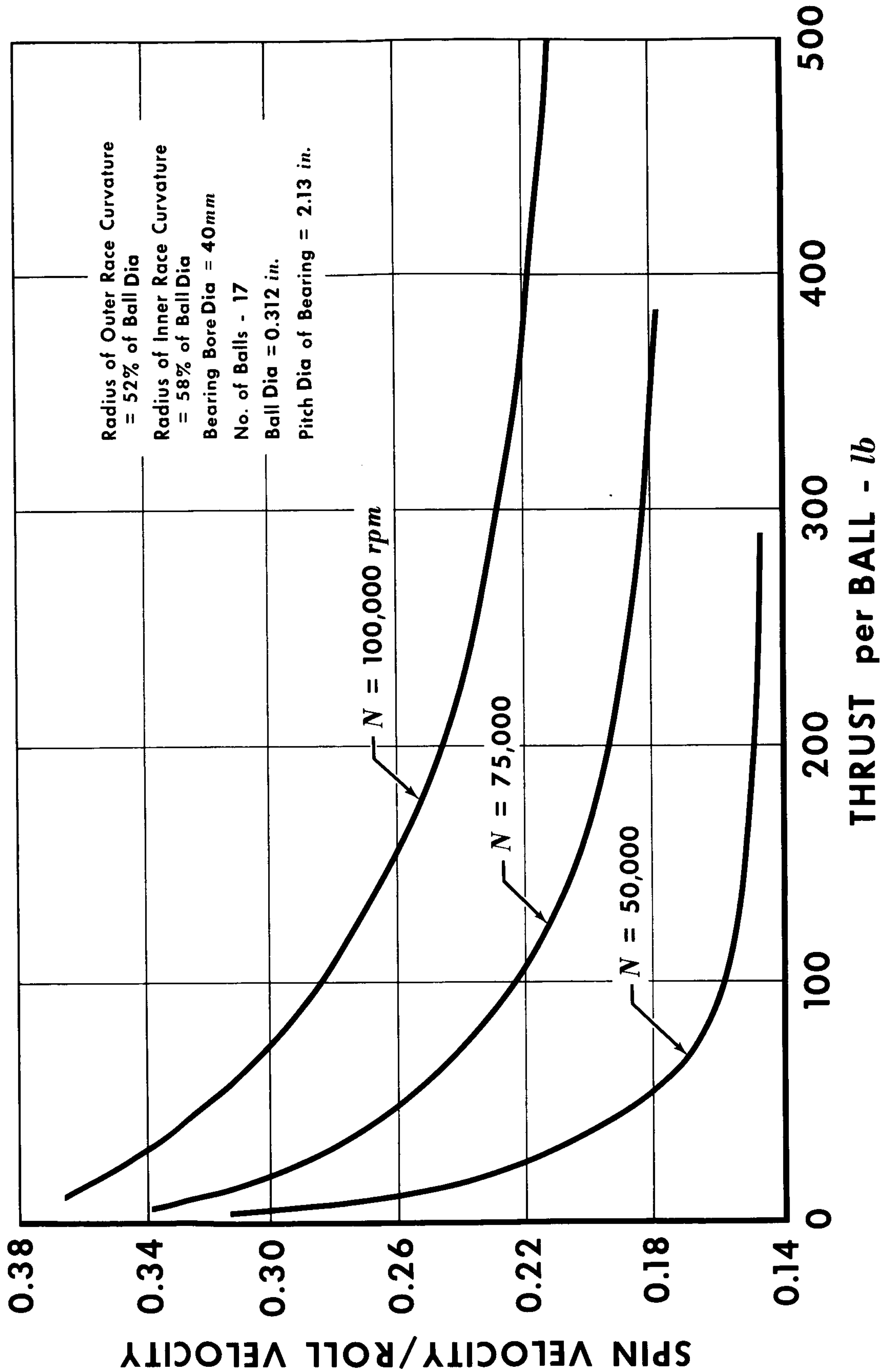

Figure II-10. Ratio of Spin Velocity and Roll Velocity vs Thrust Per Ball

FD 6731

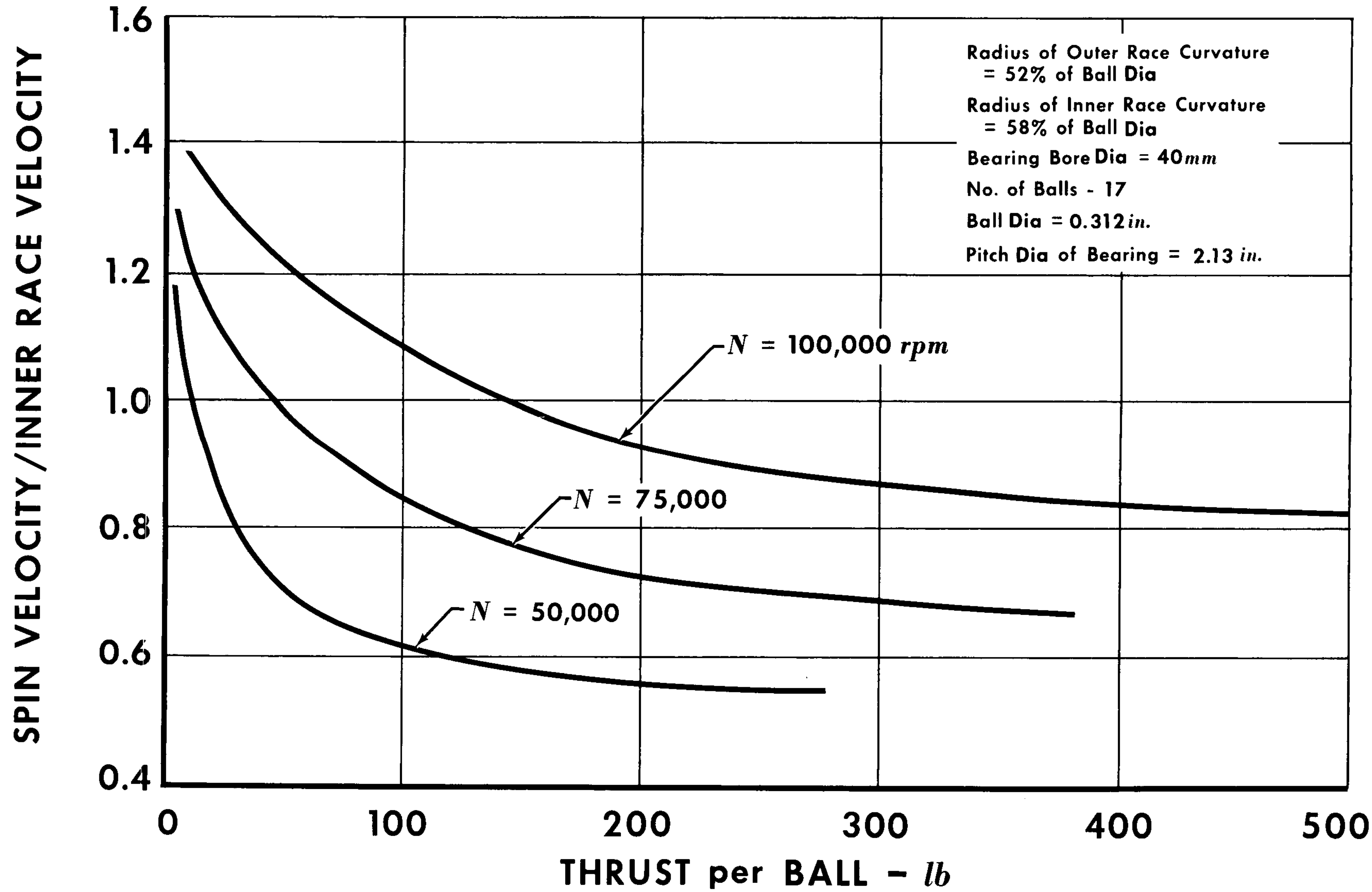

Figure II-11. Ratio of Spin Velocity and Inner Race Velocity vs Thrust Per Ball FD 6732

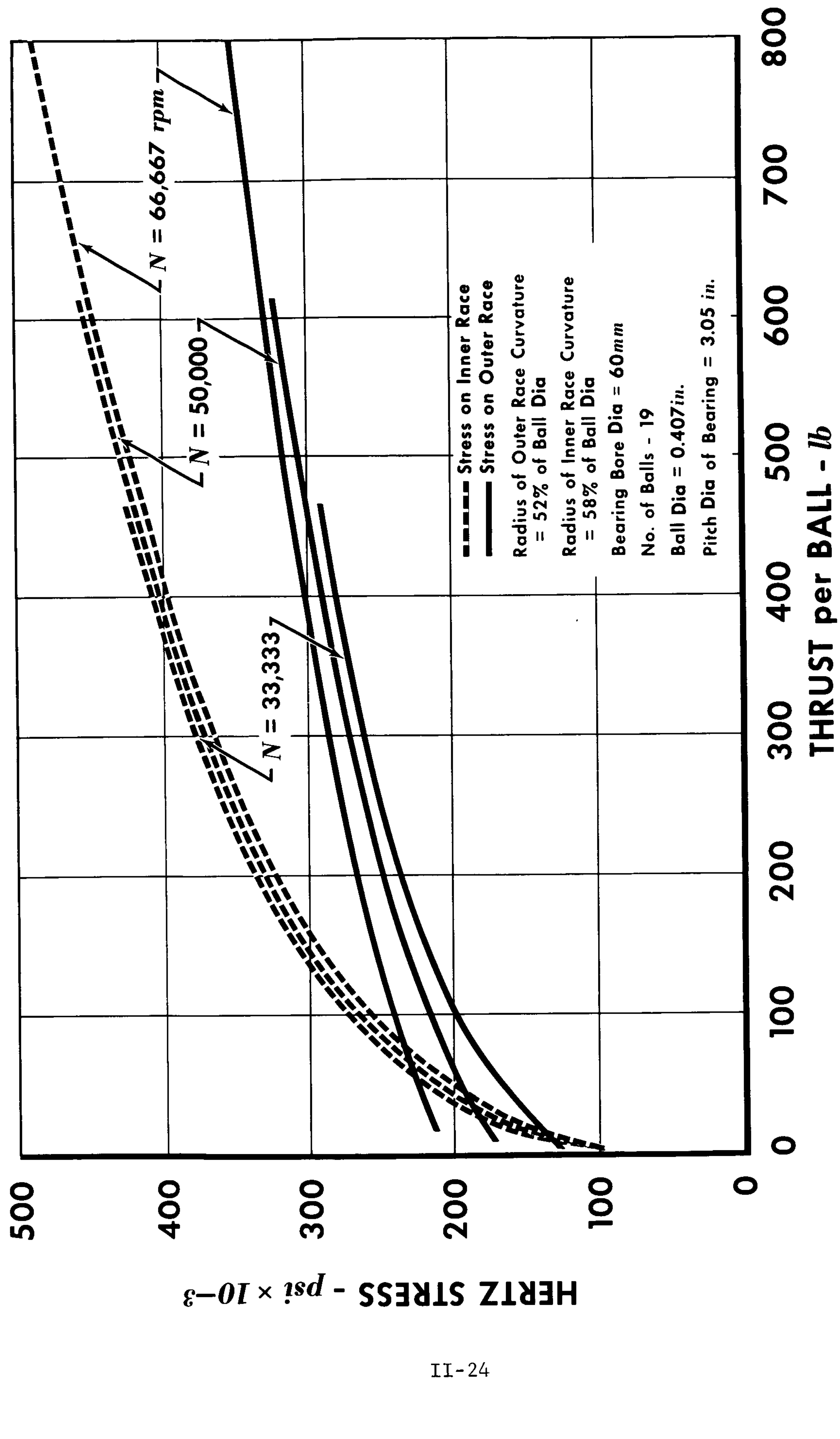

Figure II-12. Hertz Stress vs Thrust Per Ball

FD 6733

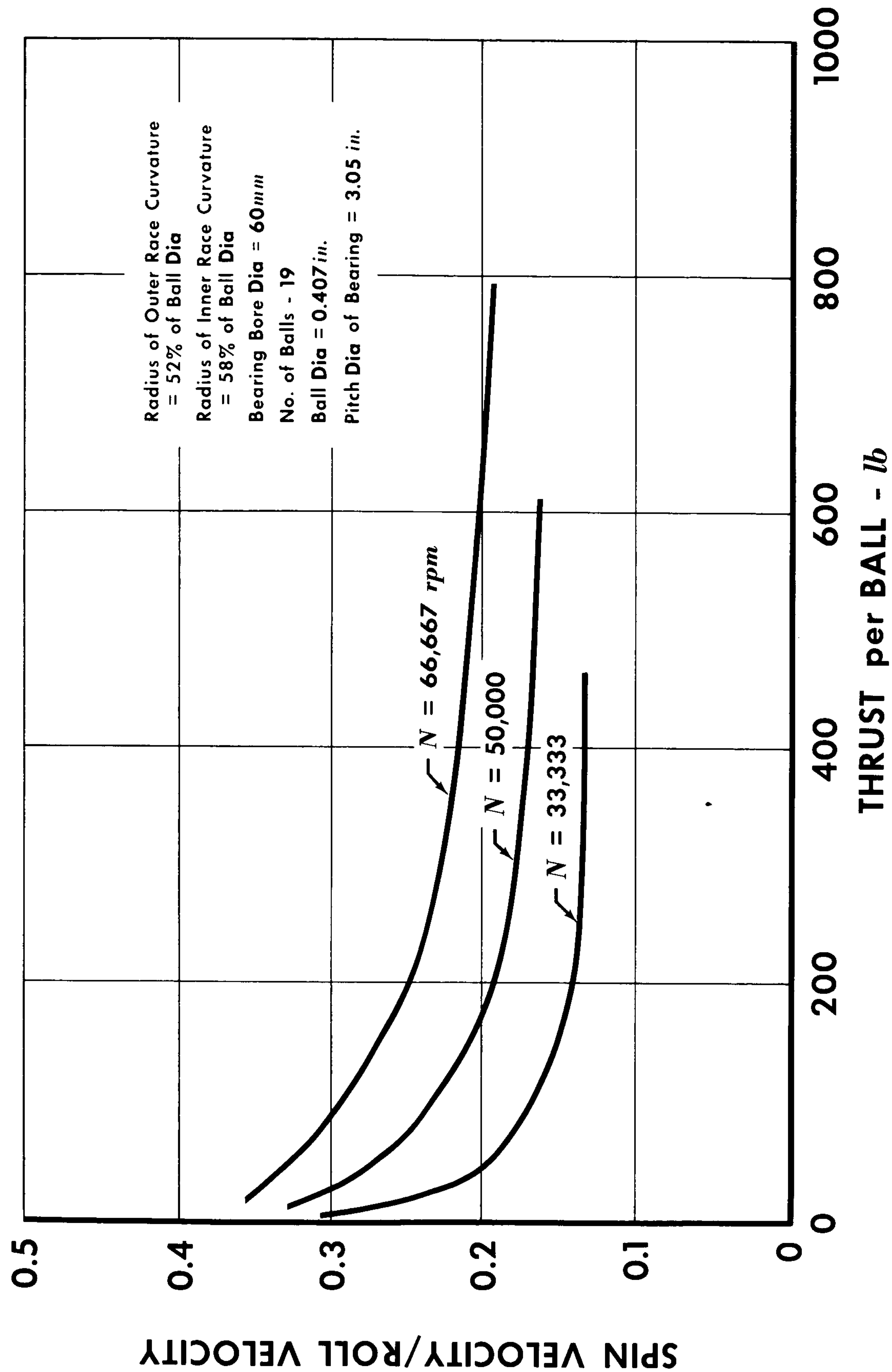

Figure II-13. Ratio of Spin Velocity and Roll Velocity vs Thrust Per Ball

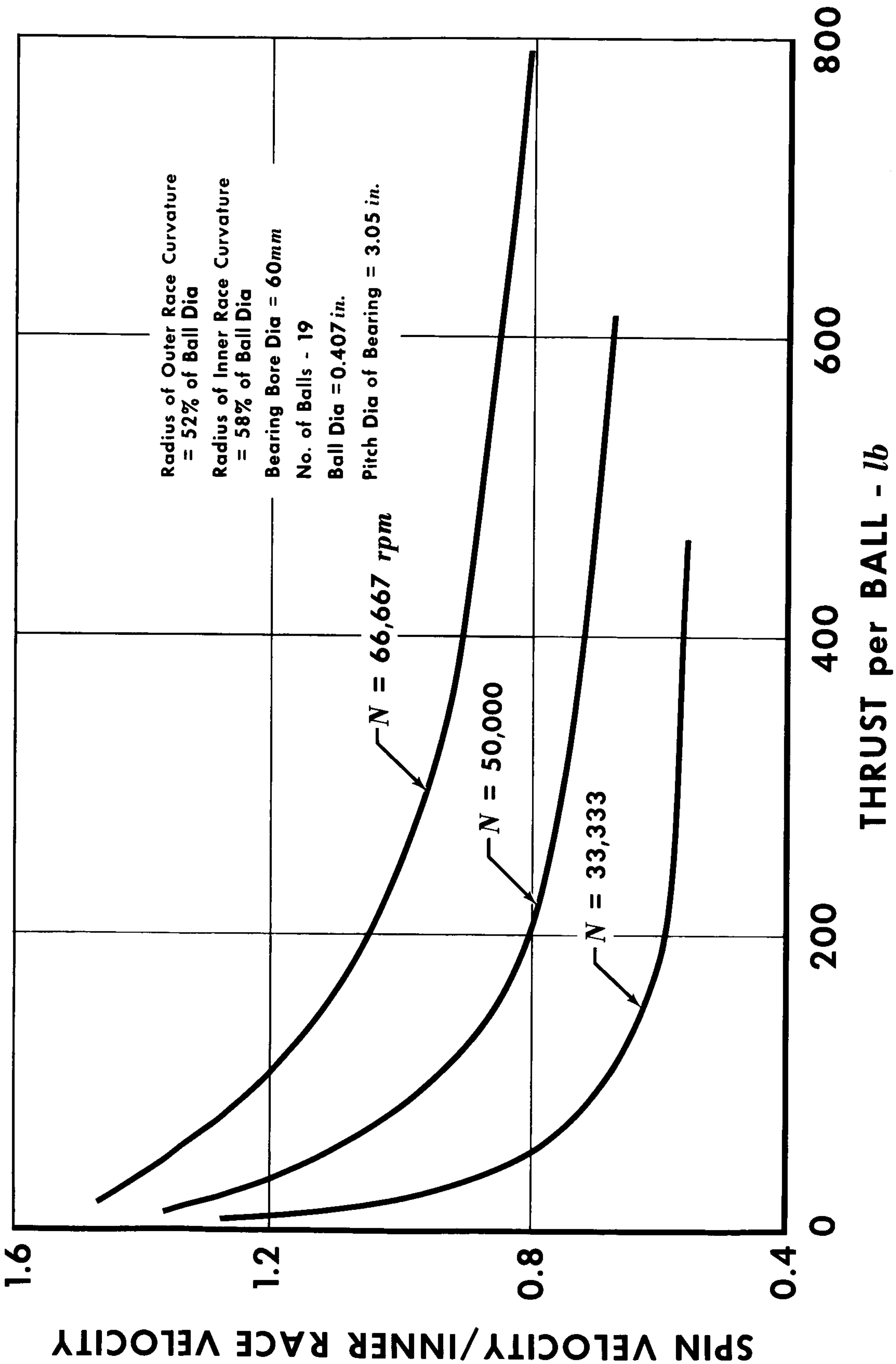

FD 6735

Figure II-14. Ratio of Spin and Inner Race Velocity vs Thrust Per Ball

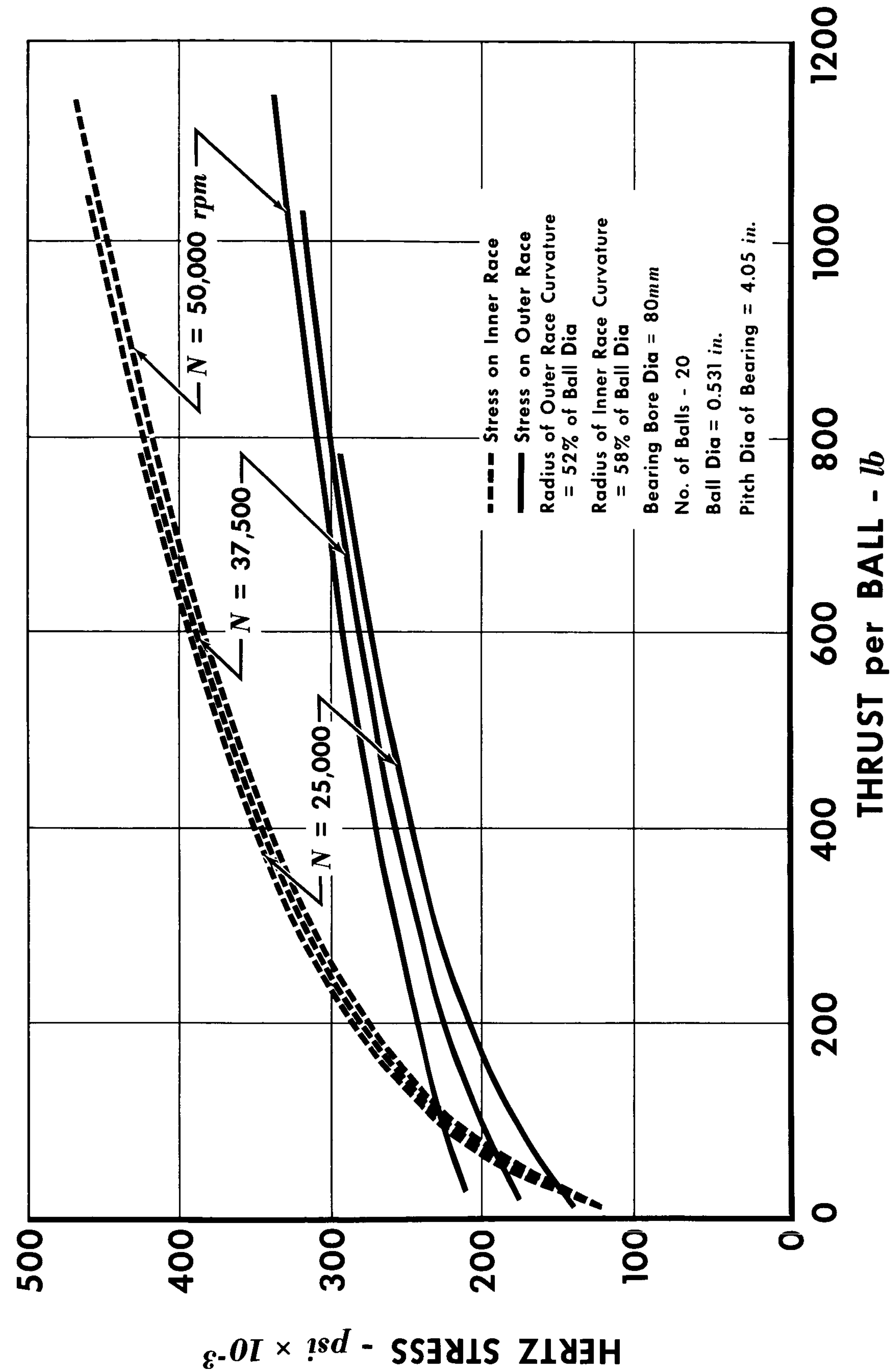

FD 6737

Figure II-15. Hertz Stress vs Thrust Per Ball

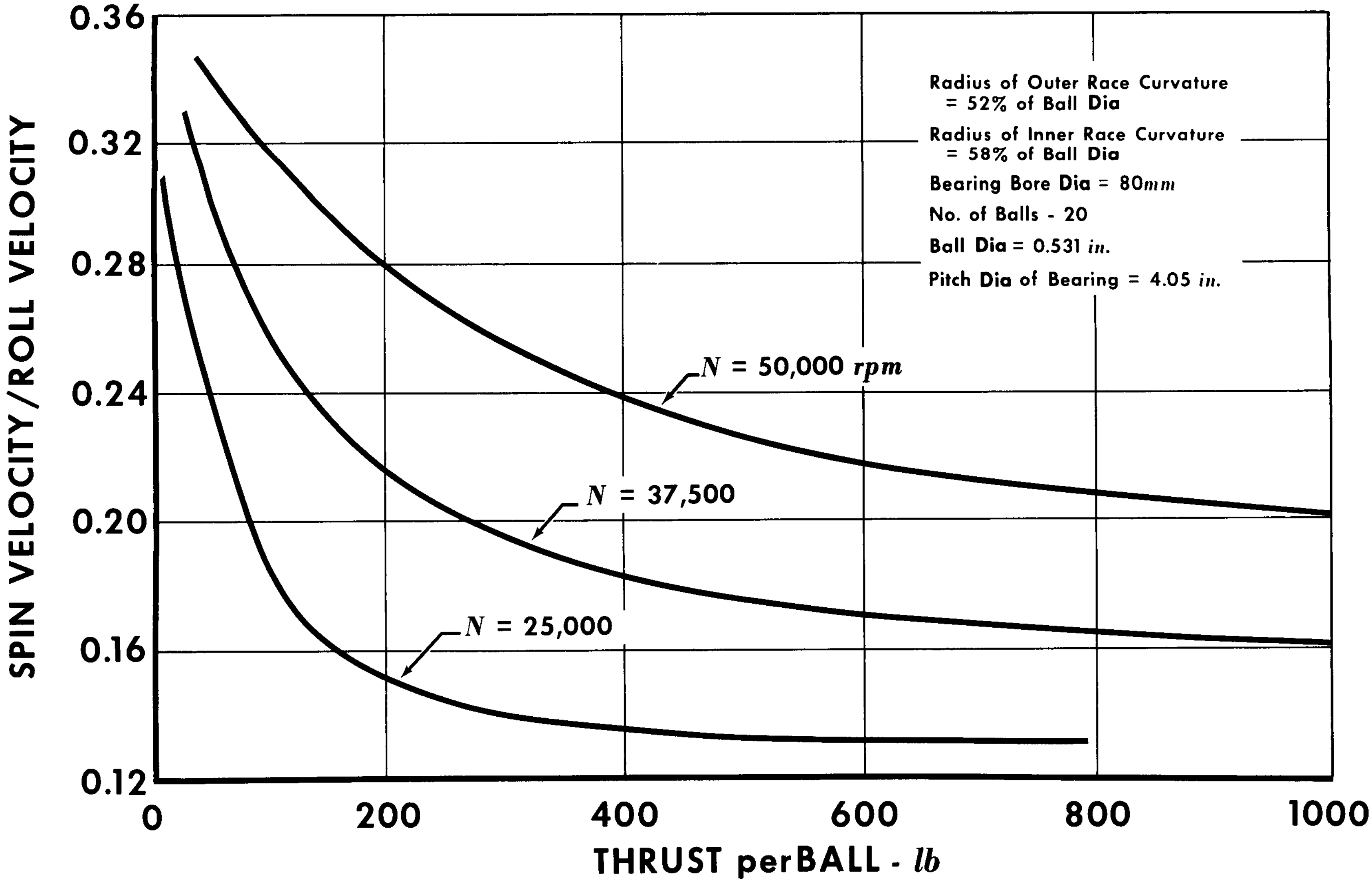

Figure II-16. Ratio of Spin Velocity and Roll Velocity vs Thrust Per Ball FD 6738

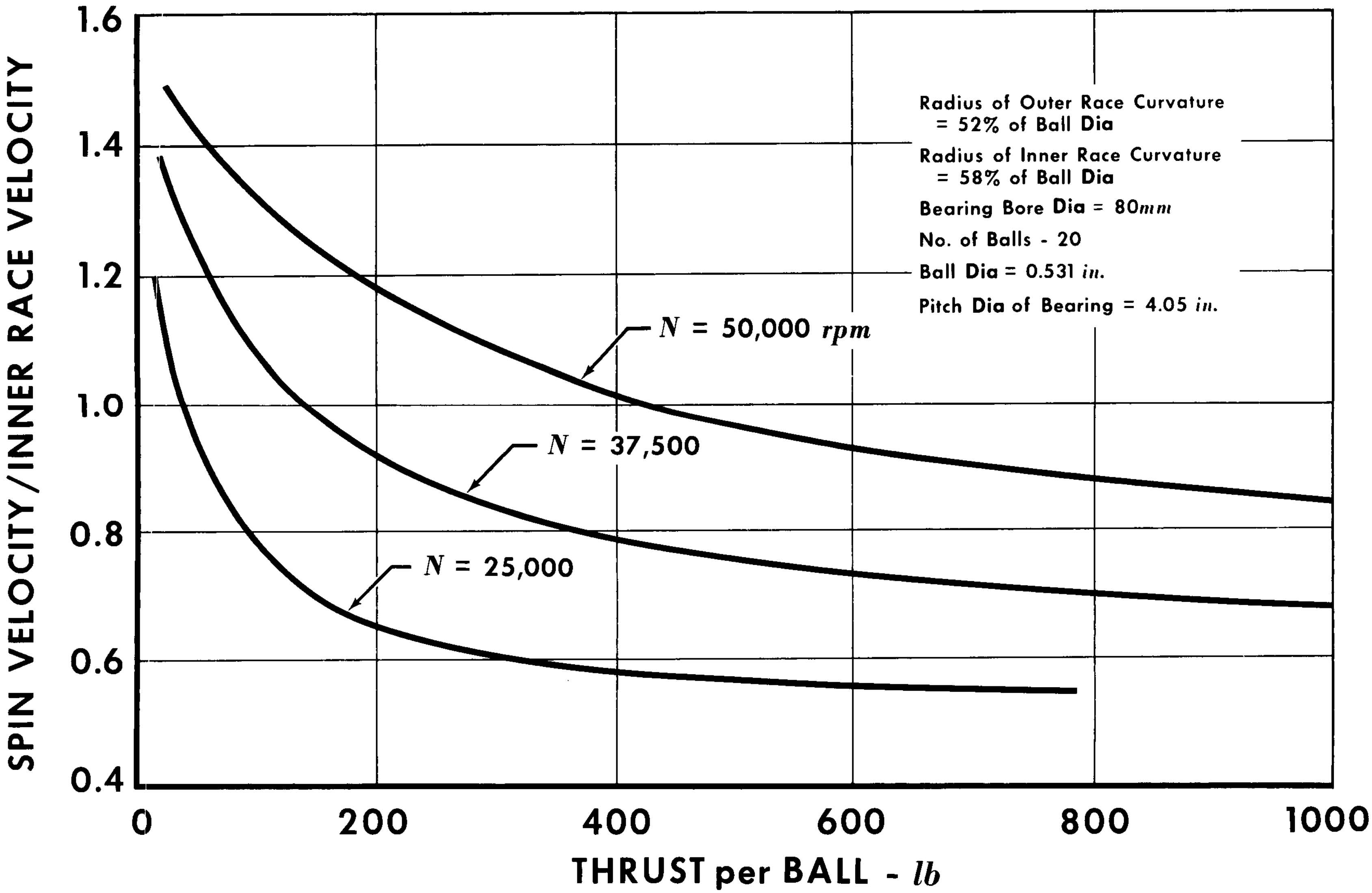

Figure II-17. Ratio of Spin Velocity and Inner Race Velocity vs Thrust Per Ball FD 6739

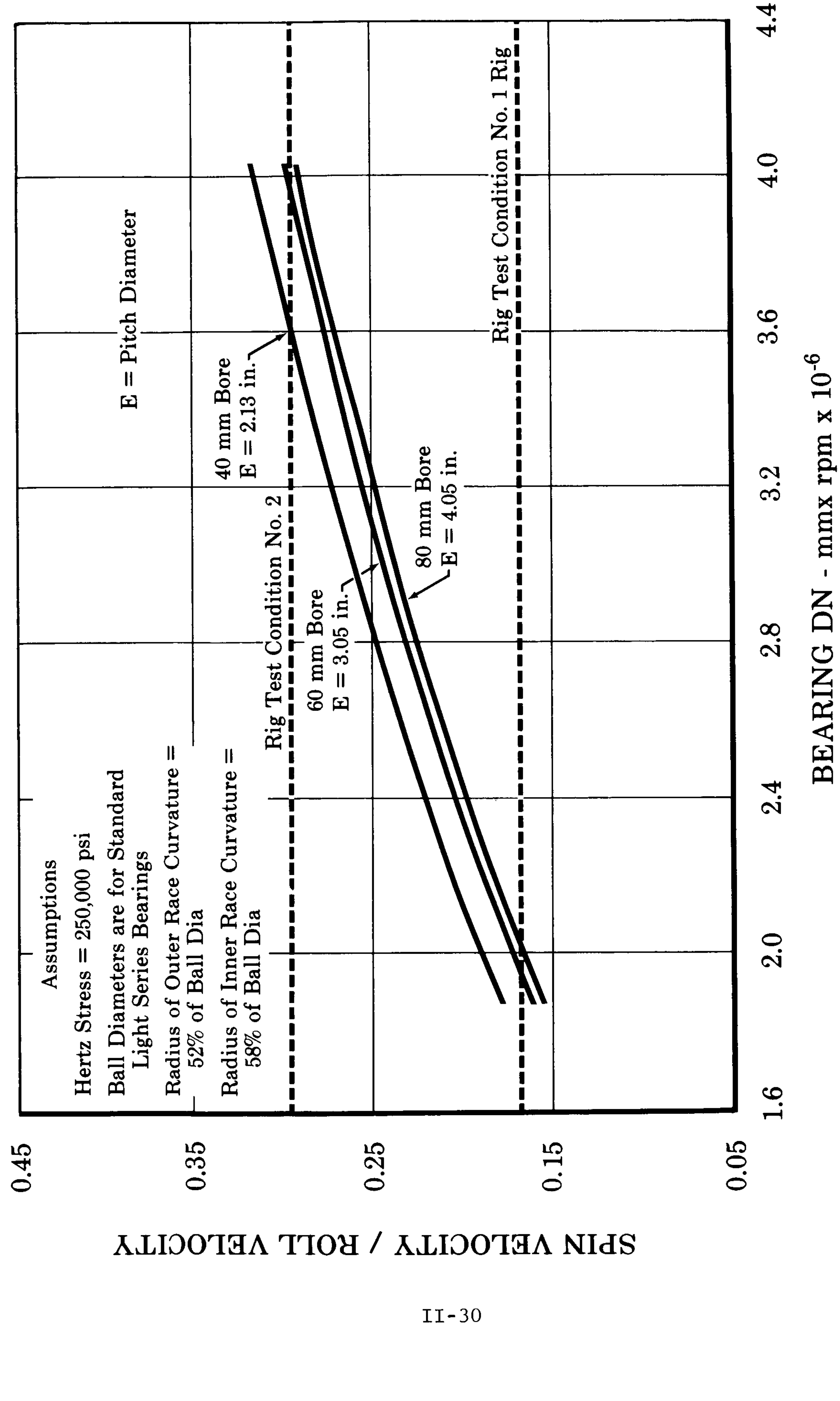

FD 6740A

Figure II-18. Effect of DN on Ratio of Spin Velocity to Roll Velocity

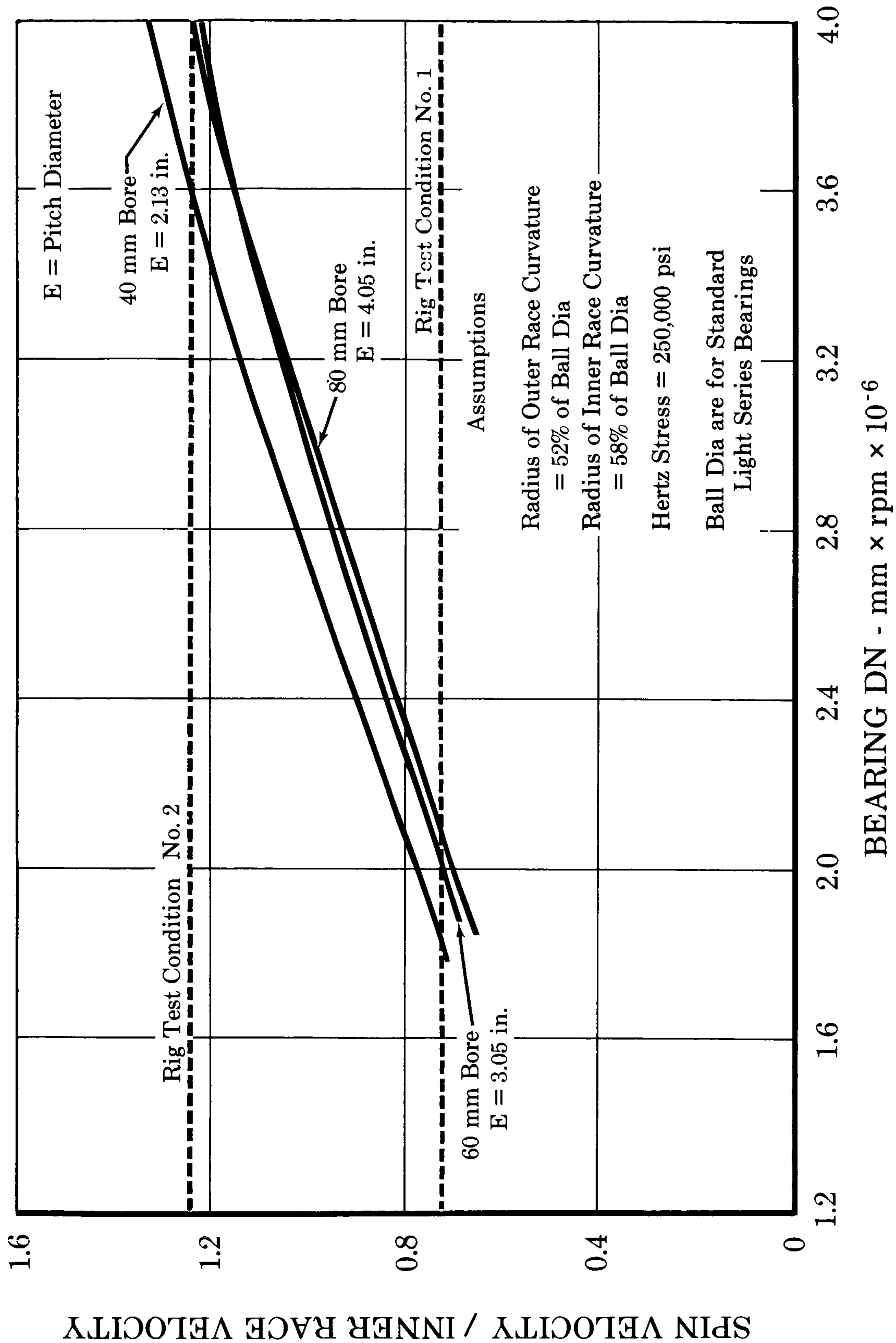

Figure II-19. Effect of DN on Ratio of Spin Velocity to Inner Race Velocity

FD 6741A

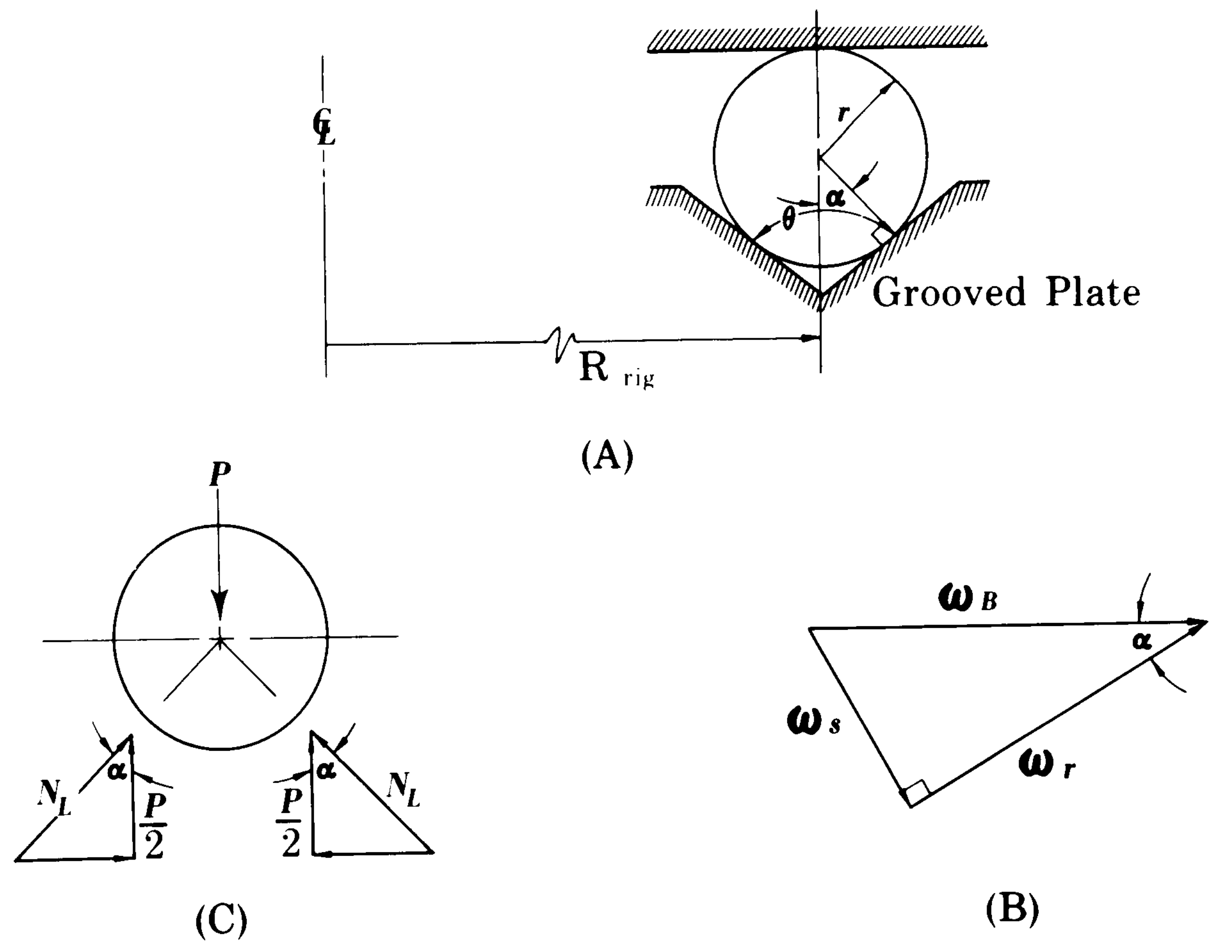

Figure II-20. Angular and Vectorial Relationships for Ball-Plate Test Apparatus FD 6729A

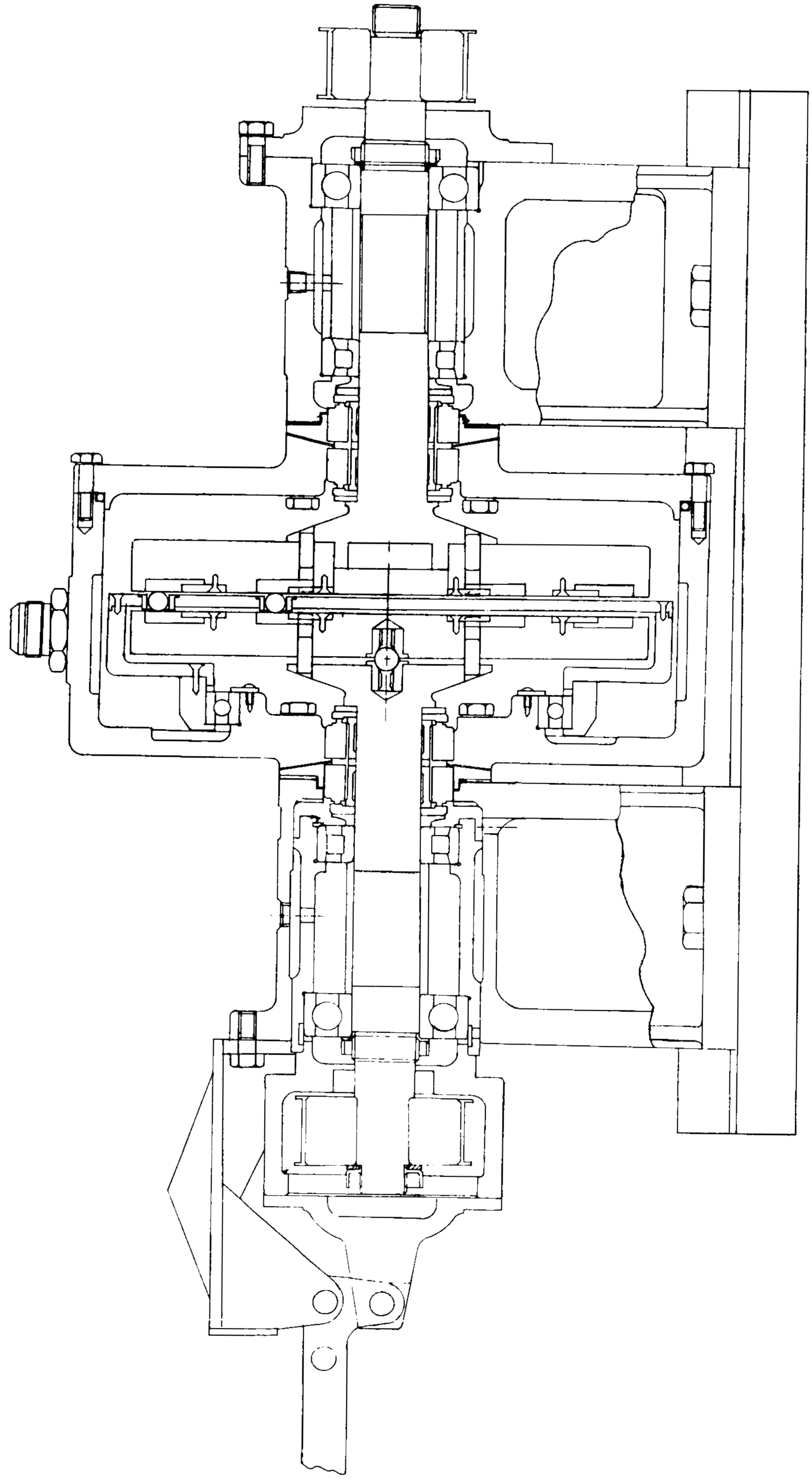

FD 6728

Figure II-21. Ball-Plate Test Apparatus

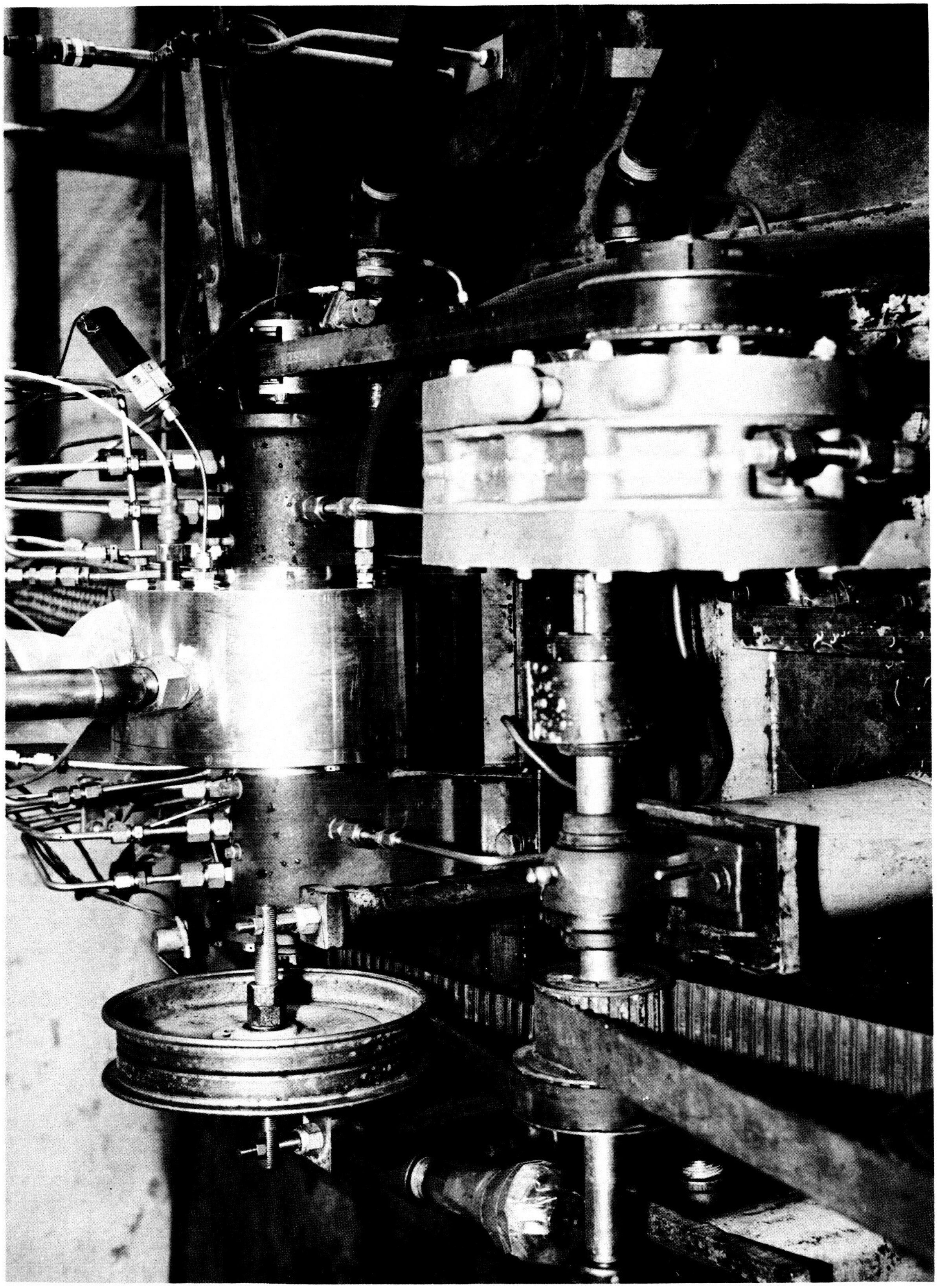

FE 41558

Figure II-22. Overall View of Ball-Plate Test Apparatus

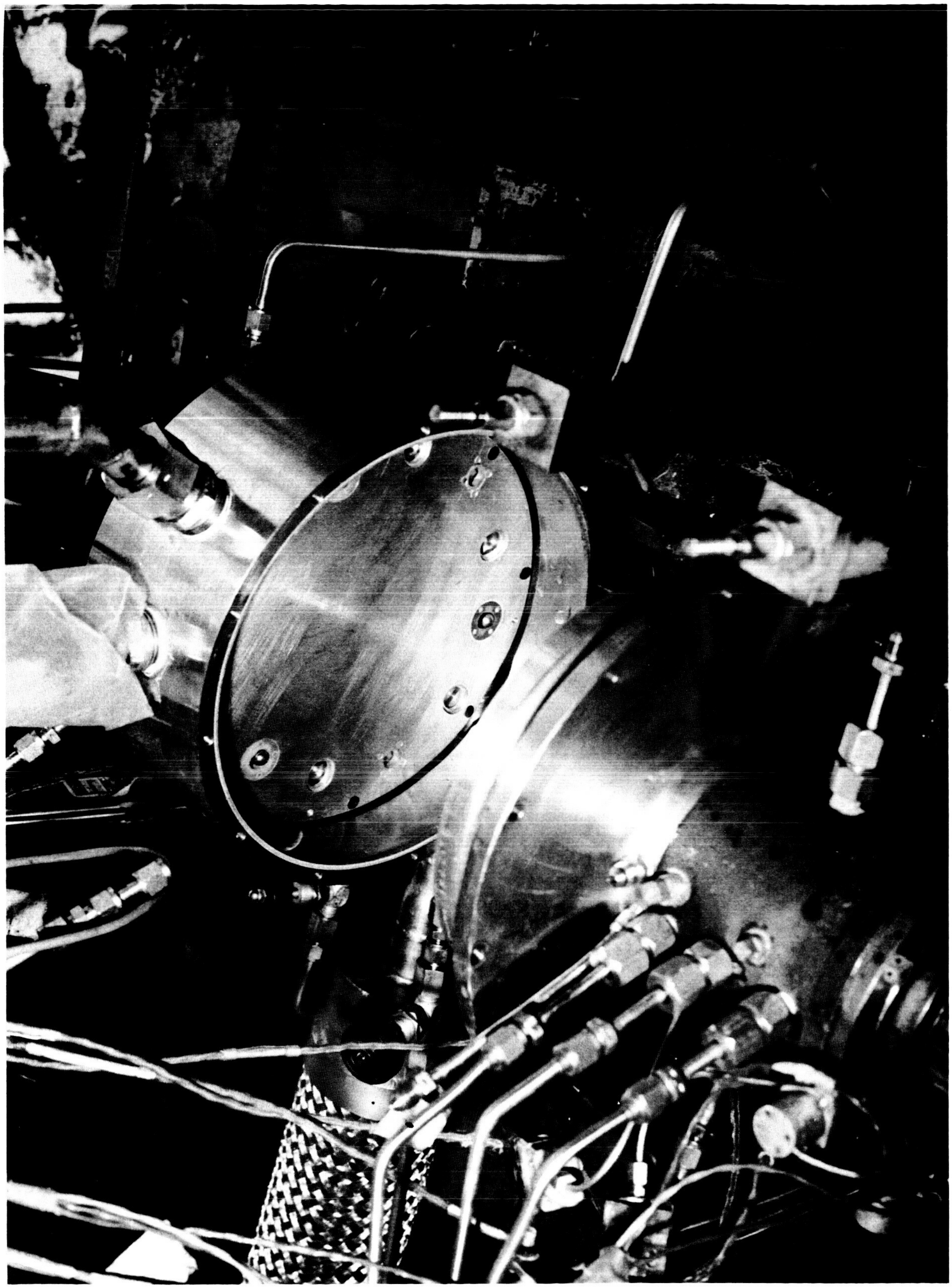

FE 41559

Figure II-23. Close-up of Ball-Plate Test Apparatus

SECTION III
SELECTION AND TESTS OF STANDARD MATERIALS

The purpose in the experimental evaluation of standard material combinations was to establish a basic level of performance to which subsequent tests of candidate materials could be compared.

The standard materials chosen for this portion of the experiment were:

1. AISI 440C balls and plates with Rulon A retainer inserts. Rulon A is a silicon-filled fluorocarbon composition.
2. AISI 440C balls and plates with DU retainer inserts. (DU is the trade name for a sintered matrix of bronze micropowder, the pores of which are filled with a lead-fluorocarbon mixture. The composite is backed with a thin steel strip.)

The first standard (Rulon A inserts) material has been used successfully for several years in the RL10 liquid hydrogen/oxygen engine's turbopumps and gearboxes. The second standard has been tested at DN values in excess of 2×10^6 mm-rpm in an advanced high pressure hydrogen pump at the Florida Research and Development Center.

Each standard material was subjected four times to each of the two test conditions established in Section II of this report and shown in table II-1. The results of these tests are presented in table III-1.

All four specimens using the Rulon A retainer inserts successfully completed 10 hours at an equivalent DN value of 2×10^6 mm-rpm. In all cases, macrographic inspection showed the balls and races to be in excellent condition. The wear in the retainer insert pocket was low and the vibration amplitude indicated by the accelerometer on the loading

Table III-1. **Standard Material Test**

Test No.	Date	Equivalent DN (10^6 mm-rpm)	Time (Hours)	Materials	Remarks
1	1-24-64	4	0.2	Retainer: DU Balls & Races: AISI 440C	Retainer Wear: Low Balls & Races: Fatigued spot found on one ball
2	1-24-64	2	1.6	Retainer: DU Balls & Races: AISI 440C	Retainer Wear: High plus Breakage Balls & Races: Badly damaged Insert failed mechanically
3	1-29-64	4	2.1	Retainer: Rulon A Balls & Races: AISI 440C	Retainer Wear: Low Balls & Races: Good after 2 hours Failed races 3 minutes after a restart Races showed signs of fatigue
4	1-31-64	2	10.0	Retainer: Rulon A Balls & Races: AISI 440C	Retainer Wear: Low Balls & Races: Good Condition
5	2-4-64	4	4.5	Retainer: Rulon A Balls & Races: AISI 440C	Retainer Wear: High Balls & Races: Fatigued
6	2-10-64	2	10	Retainer: Rulon A Balls & Races: AISI 440C	Retainer Wear: Low Balls & Races: Good Condition
7	2-10-64	4	0.3	Retainer: DU Balls & Races: AISI 440C	Retainer Wear: Low Balls & Races: Good Condition
8	2-11-64	2	10.0	Retainer: DU Balls & Races: AISI 440C	Retainer Wear: Moderate Balls & Races: Good Condition
9	2-12-64	4	5.75	Retainer: Rulon A Balls & Races: AISI 440C	Retainer Wear: Low Balls & Races: Fatigued

Table III-1. Standard Material Test (Continued)

Test No.	Date	Equivalent DN (10^6 mm-rpm)	Time (Hours)	Material	Remarks
10	2-12-64	2	10	Retainer: Rulon A Balls & Races: AISI 440C	Retainer Wear: Low Balls & Races: Good Condition
11	2-13-64	4	10	Retainer: Rulon A Balls & Races: AISI 440C	Retainer Wear: Low Balls & Races: Good Condition
12	2-13-64	2	10	Retainer: Rulon A Balls & Races: AISI 440C	Retainer Wear: Low Balls & Races: Good Condition
13	2-13-64	4	4.66	Retainer: DU Balls & Races: AISI 440C	Retainer Wear: Moderate Balls & Races: Good Condition
14	2-17-64	2	10.0	Retainer: DU Balls & Races: AISI 440C	Retainer Wear: Low Balls & Races: Good Condition
15	2-18-64	4	0.13	Retainer: DU Balls & Races: AISI 440C	Retainer Wear: Low Balls & Races: Good Condition
16	2-18-64	2	10.0	Retainer: DU Balls & Races: AISI 440C	Retainer Wear: Low Balls & Races: Good Condition

arm was approximately .3 mils. The loading arm magnifies the axial oscillation of the plates by a factor of 6. As discussed earlier, the tests were stopped after 10 hours (a condition specified by the contract) since a 10-hour life is compatible with most current and advanced liquid rocket engine lives.

Three of the four specimens using DU retainer inserts successfully completed 10 hours at an equivalent DN value of 2×10^6 mm-rpm. The test of the fourth specimen was aborted after 1.6 hours. Failure was attributed to a fractured DU insert. In all other cases, the wear in the insert pockets was moderate. In general, the surfaces of the DU races and balls appeared to be slightly rougher than found in the Rulon A standard combinations. The surface roughness has been attributed to bronze particles from the DU insert being pressed into the plate surface. The balls and plates were bronze-colored after each test.

Figure III-1 shows that the Rulon A insert specimens exceeded the performance of the DU insert specimens at an equivalent DN values of 4×10^6 mm-rpm . The wear in the pockets of the Rulon A inserts was low as compared to moderate wear of the DU inserts, but higher than observed after the low DN tests. Figures III-2 through III-7 show low and high magnification photographs taken of typical surface spalling, and retainer insert wear resulting from tests conducted in this portion of the experimental program.

Based on the results of these tests the material combination of Rulon A inserts and AISI 440C balls and races was chosen as the primary standard, and the minimum level of performance which the candidate material must meet has been determined as follows.

1. Satisfactorily complete 10 hours of operation (2 tests) at an equivalent DN value of 2×10^6 mm-rpm.
2. Satisfactorily complete a minimum of 5 hours at an equivalent DN value of 4×10^6 mm-rpm.
3. Retainer insert wear must be no greater than experienced in the standard tests.

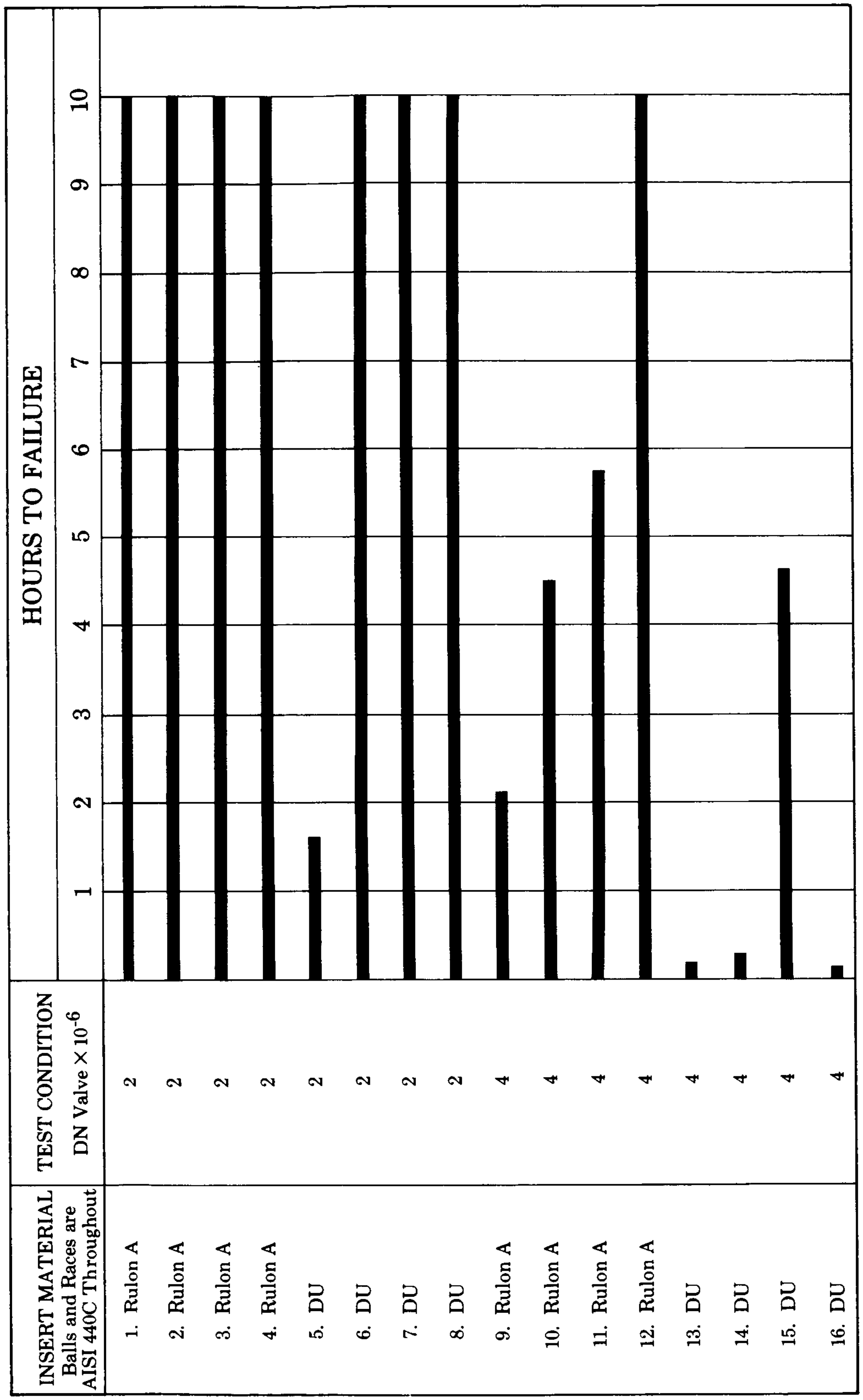

FD 8194

Figure III-1. Summary of Bearing Lubricant Test Results

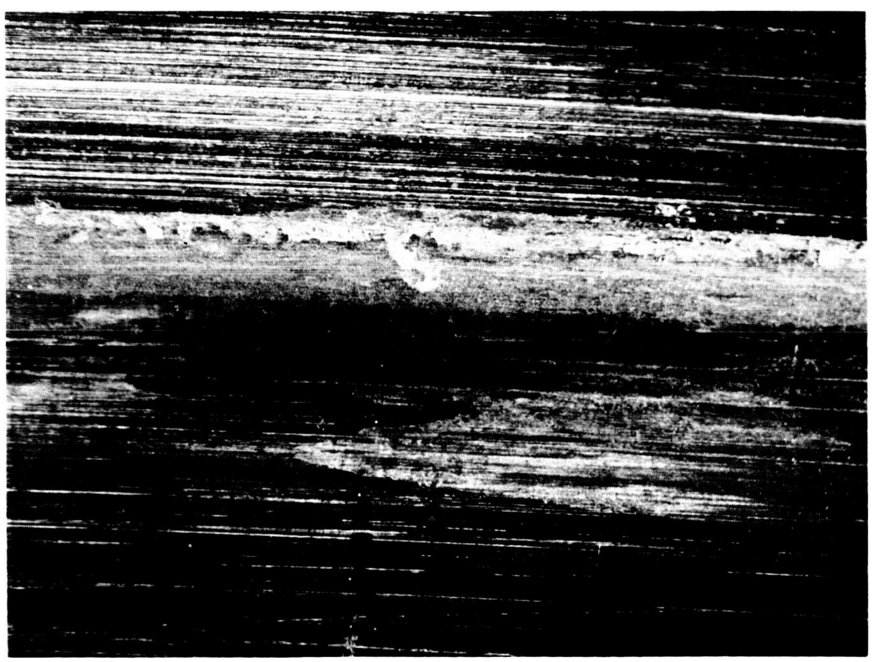

Figure III-2. View of Wear Path in Outer "V" Showing Most Severe Pitting Present on the Part. (Test No. 3, Rulon A at DN = 4 x 10^6 mm-rpm) FL 3530

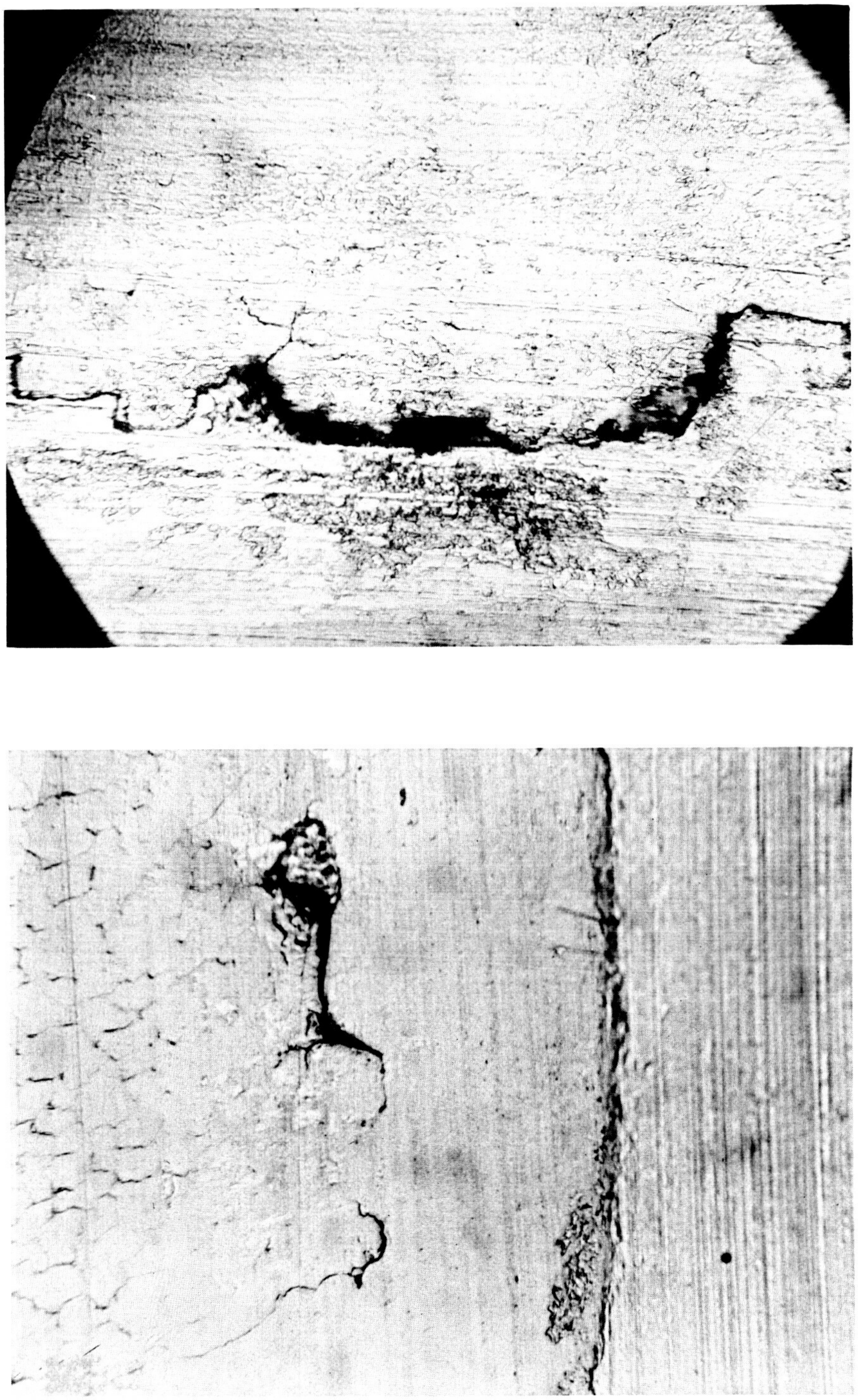

Figure III-3. View of Typical Spalls in Wear Path. Photos were taken from Chromium Shadowed Replicas. (Test No. 3, Rulon A at DN = 4×10^6 mm-rpm)

FM 6069

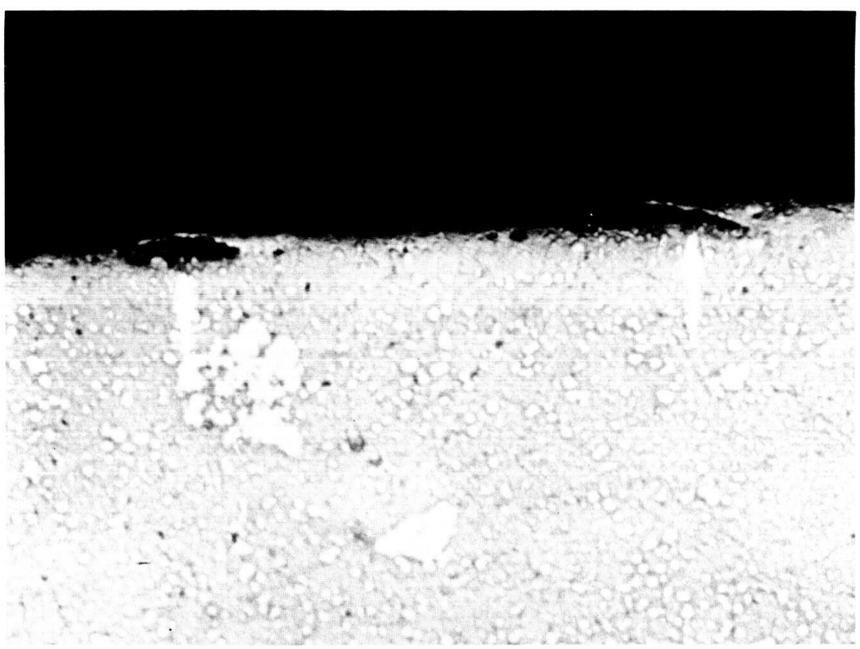

Figure III-4. View of Circumferential Section Through the Inner Wear Path of the Outer "V" Showing Typical Spalls. Material is AISI 440C. (Test No. 3, Rulon A at DN = 4×10^6 mm-rpm) FM 6026

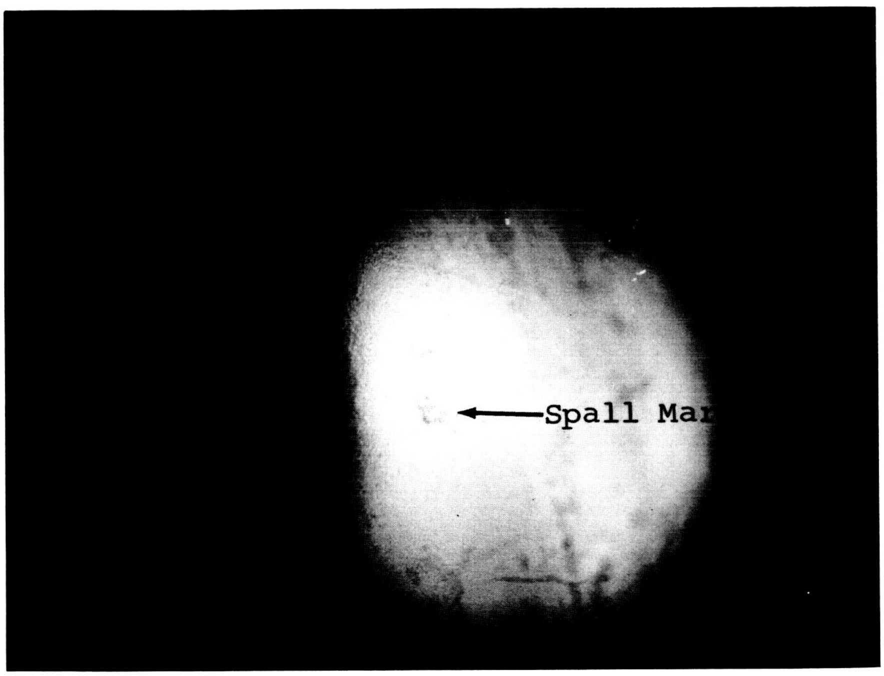

Figure III-5. Typical Surface Spalling (Rulon A after 2.6 Hours at DN = 4×10^6 mm-rpm, mag = 30X) FL 3516

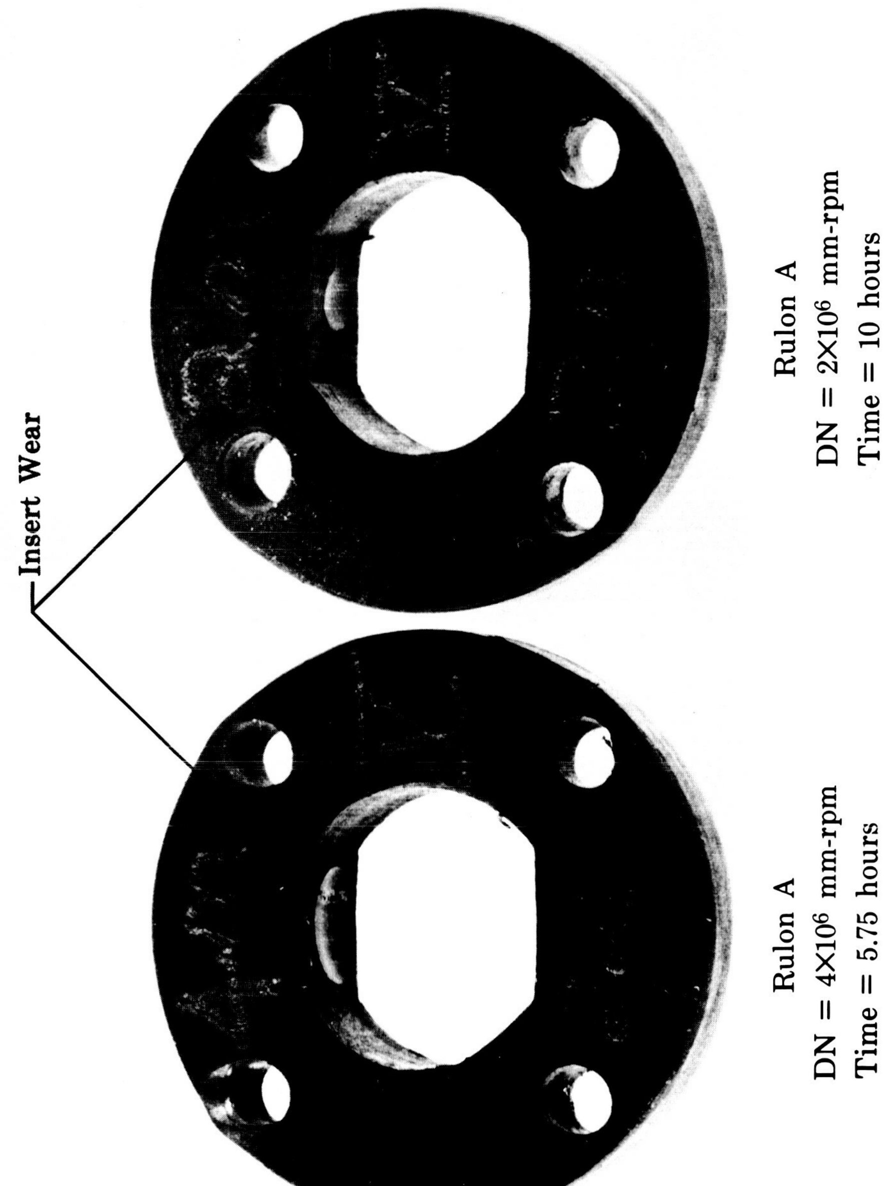

FD 8193

Figure III-6. Typical Unshrouded Insert Wear

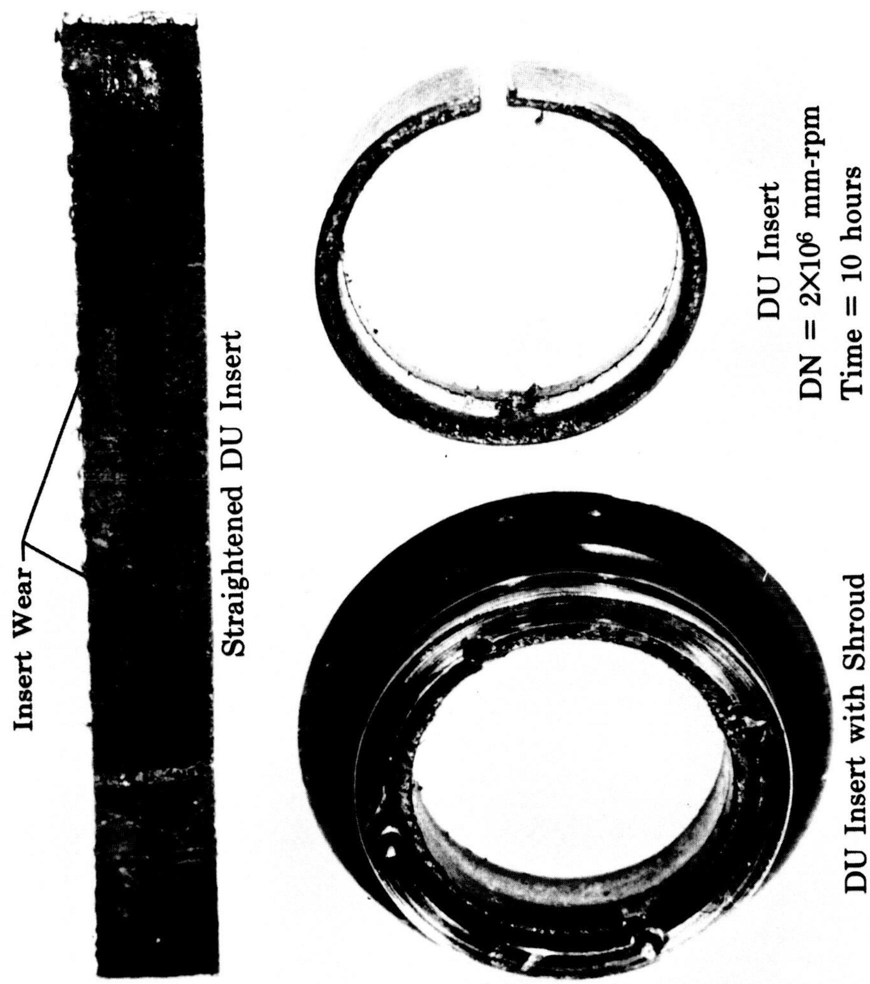

FD 8191

Figure III-7. Typical Shrouded Insert Wear

SECTION IV
SELECTION OF CANDIDATE LUBRICANT MATERIALS

The general purpose of lubrication is to increase the life of the bearing. Referring to the theory of failure discussed in Section II, the specific purpose of the lubricating material is to prevent surface damage and subsequent reduction in the fatigue life of the bearing material.

In more typical bearing applications the lubricant is usually in the form of a liquid hydrocarbon oil that either completely surrounds the bearing or is injected on the bearing with jets. In a cryogenic bearing the use of such liquid lubricants is impossible since the operating temperature is lower than the freezing point of these oils. The use of solid lubricants is,therefore, the only method available for lubrication of bearings operating in liquid hydrogen.

On the other hand the liquid hydrogen has all the characteristics of an excellent coolant. In its liquid condition, it is extremely cold (-423°F), has a high specific heat, and has a low viscosity.

To summarize, ball bearings operating in liquid hydrogen are (1) cooled by the hydrogen and (2) lubricated by some solid lubricant.

Because of the low viscosity of hydrogen, the bearings can be completely submerged without any concern about the viscous drag forces on the moving parts. On the other hand, the problem of supplying the lubricant is not so straightforward. Possible methods include (1) dry-film lubricants bonded to the raceways,

(2) metallized or flame-sprayed wear-resistant raceways, (3) injected nonmetallic submicron size powders, or (4) retainer materials that have inherent self-lubricating characteristics. In the first two methods, the lubricant is part of the bearing wear surfaces and in the third method it is carried by the coolant to the wear surfaces. In the fourth method, a thin lubricating film is transferred by the balls from the retainer to the raceways. This thin film then serves as the load-carrying lubricant for the wear surface. It was initially decided that all four of these methods of lubricating liquid hydrogen-cooled ball bearings would be investigated in this program.

A literature survey (see Bibliography) was conducted to determine the most likely candidate in each of the four categories. This study revealed the fact that possible "packing" problems associated with powder injection devices would greatly hinder the success of the lubrication mode. As a result no candidates that were representative of this lubrication method were selected. This study on the other hand, resulted in the following selections.

1. Lubricating Retainer Materials
   a. AMS 5630 balls and plates with Salox M retainer inserts. Salox M is fluorocarbon matrix filled with 40% (by weight) bronze.
   b. AMS 5630 balls and plates with Salox Z-1 retainer inserts. Salox Z-1 is a fluorocarbon matrix filled with 15% (by weight) molybdenum disulphide (MoS_2).

c. AMS 5630 balls and plates with retainer inserts made of a polyimide filled with 15% (by weight) MoS_2.

d. AMS 5630 balls and plates with retainer inserts made of a silver matrix filled with 20% (by volume) MoS_2.

e. AMS 5630 balls and plates with retainer inserts made of a silver matrix filled with 20% (by volume) calcium fluoride (CaF_2).

f. AMS 5630 balls and plates with inserts made of an aluminum matrix filled with the more effective of the two lubricant fillers used in item (d) and (e), preceding.

g. AMS 5630 balls and plates with inserts made of boron nitride (not pyrolytic).

2. Lubricants Bonded to Plates

a. AMS 5630 balls, AMS 5630 plates plated with modified MLF-5 dry film lubricants, and retainer inserts made of Rulon A. MLF-5 consists of graphite, gold, MoS_2, and a sodium silicate ($Na_2O \cdot 2.9\ SiO_2$) binder.

b. AMS 5630 balls, AMS 5630 plates plated with a fluorocarbon compound, Fluoroglide. Fluoroglide is a fluorocarbon telomer manufactured by Chemplast, Inc.

3. Plated Wear Resistant Raceways

AMS 5630 balls, AMS 5630 plates plated with tungsten carbide (metallized).

Notice the category related to injected nonmetallic sub-micron size powder was not included in the list of candidate lubricating systems. This method was eliminated when the literature search revealed that the beneficial characteristics of this lubrication mode would be overshadowed by possible "packing" problems associated with injection devices.

The various candidate lubricants listed above were selected for the following reasons.

The RL10 rocket engine performs reliably with ball bearings operating in liquid hydrogen by using retainers made of Rulon A, a silicon-filled fluorocarbon composite. In view of this success, it was decided to explore other fluorocarbon composities, with emphasis on improved filler materials. Salox M (a bronze-filled fluorocarbon matrix) and Salox Z-1 (a MoS_2-filled fluorocarbon matrix) both were expected to provide increased resistance to deformation, low coefficient of friction, increased wear resistance, and higher strength/weight ratios than Rulon A.

One company recently published information relating to a polyimide called Vespel. This organic polymer theoretically offers much higher strength/weight ratios than any of the filled fluorocarbon matrices and can be filled with either graphite or MoS_2. The MoS_2 filler is generally considered preferable for exposure to a vacuum environment compared to graphite, which depends on water vapor to act as a lubricant. The same trends are expected to remain true for a reducing atmosphere such as hydrogen.

The success of the nonmetallic composite retainer materials has prompted some investigations of metallic composites filled with lubricating materials. Metallic composites provide higher strength/ weight ratios and in some cases eliminate the requirements for retainer shrouds to withstand high retainer rotating stresses. In addition most metallic composites would not be damaged in nuclear environments. Some success has been reported with metal composites using a silver matrix with the sulfides, tellurides, and selenides of molybdenum and tungsten. A small amount of tetrafluoroethylene (TFE) has in some cases been added in the structure. In general, there appears to be no advantage to using molybdenum-diselenide ($MoSe_2$), tungsten disulfide (WS_2), or tungsten-ditelluride (WTe_2) instead of MoS_2. In addition, some success has been reported with CaF_2 as a lubricant. In view of the reported previous experience, MoS_2 and CaF_2 were chosen as the filler materials for the candidate metal matrices for use in this program. The final choice in this category was the selection of the metal matrix itself. Due to the high thermal conductivity and the amount of experience compiled in manufacturing silver composites, this material was selected instead of nickel or copper. However, silver does not provide a strength/weight ratio that is sufficient to eliminate the use of retainer structural shrouds for use in high DN bearings. For this reason, aluminum with its high strength/weight ratio was chosen as a second matrix material. A retainer made with an aluminum matrix would not have to be shrouded in most applications. It was decided that the filler for the aluminum composite would be the most effective lubricant resulting from the tests of the MoS_2-filled silver composite and the CaF_2-filled silver composite.

The dry film lubricant, MLF-5, has been used successfully in various applications at NASA and Pratt & Whitney Aircraft (RL10 gimbal lubricant). No information is available to indicate that MLF-5 has been used in high speed ball bearings. However, success with the gimbal tests indicates it would be a worthwhile candidate for the existing program.

Boron nitride was substituted for the injected fluorocarbon powder method which was eliminated early in the program and which is discussed above. The material is commonly known as white carbon and is sometimes used as nose pieces in cryogenic rotating shaft seals. It theoretically has an excellent coefficient of friction and wear resistance.

In view of the theory that cryogenic bearings used in the RL10 are lubricated by Rulon A which is transferred from the retainer to the raceway by the balls, it follows that the more direct approach would be to plate the raceways with a fluorocarbon (the principal component in Rulon A) in the manufacture of the race. The difficulty in this method is in achieving an extremely thin fluorocarbon coating. Excessive material will foul the path of the ball and cause damage. A thin coat of Flouroglide, trade name for a fluorocarbon coating compound, was employed since this material required no curing cycle. The coating thickness was approximately .001 in.

Even through flame-spray surfaces should not be considered as lubricants as such, they do increase the wear resistance of the surface and consequently provide some assistance to the retainer lubricant in performing its job. Many types of flame-sprayed surfaces are available. For thermal compatibility with the base metal and alleged ease of manufacture, tungsten carbide was selected for this program. As discussed later in this report, the manufacture of the specimen was not successful and as a result these specimens were not tested.

SECTION V
TESTS OF CANDIDATE MATERIALS

The tests of the candidate materials are summarized in table V-1 and began with two low speed evaluations (equivalent DN value of 2×10^6 mm-rpm) of the metal composite, $Ag\text{-}MoS_2$. Test conditions were identical to those used in the 2×10^6 DN tests of the standard materials. The results of these tests were somewhat encouraging in that the candidate successfully completed 10 hours in each case, and therefore met the first requirement defined in Section III. Inspection of the balls and plates showed them to be in excellent condition. In fact, the ball tracks on the plates and the wear tracks on the balls seemed to be in better condition than when the test started. In both tests, the wear track was highly polished and contained no evidence of fatigue. On the other hand, the retainer insert was highly worn as shown in figure V-1. This level of wear would be considered unacceptable in an actual ball bearing retainer. The amount of wear with time or the wear rate is unknown. In other words it is not known whether most of the wear occurred early in the tests and leveled off as time accumulated or whether the wear rate was constant throughout the test.

Ordinarily, the wear rate demonstrated by this specimen in the low speed tests would have disqualified it for subsequent high speed tests. But the excellent lubricating characteristics demonstrated in the first two tests were considered so encouraging that a high speed test was scheduled to (1) confirm these lubricating characteristics and (2) determine if the wear rate increased with the higher ball rotational velocities. The results of the high speed test were again encouraging. The specimen successfully completed a 10-hour endurance run and post-test inspection showed the wear tracks on the balls and plates to be highly polished. Again the retainer inserts were badly worn but the amount of wear did not appear to be any worse than in the two low speed tests. It would therefore appear that the wear rate was unaffected by the higher ball rotational velocity.

The next series of tests was conducting using retainer inserts made of Ag-CaF_2 and unplated AISI 440C balls and races. In general, the performance of this specimen was very poor and since it failed to meet the first requirement established by the standard materials tests, no further tests were scheduled. Retainer insert wear for this candidate is shown in figure V-2.

It should be pointed out here that the tests of the Ag-CaF_2 tests are significant from the standpoint that they indicate that it is principally the MoS_2 in the Ag-MoS_2 candidate which made that candidate effective as a lubricant. Both the Ag-CaF_2 and the Ag-MoS_2 candidates had the same amount of lubricant by volume and therefore the same approximate amount of silver in the matrix. Since the wear rate of the Ag-MoS_2 candidate was high and the excellent lubricating characteristics can be attributed to the MoS_2, it follows that there is a good possibility that silver could be replaced with other materials to permit higher resistance to wear. It would seem important to press such an investigation since bearing applications subjected to nuclear radiation atmospheres will probably require some metallic retainer. Most plastics are not satisfactory in such an environment, particularly those where the radiation level approaches 10^5 ergs per gram (c).

Table V-1

Test No.	Candidate Materials Balls	Plates	Inserts	Equivalent DN Value x 10^6	Hours To Failure	Remarks
1	440C	440C	Ag-MoS_2	2	Time = 10 hours	Balls and plates in excellent condition. No fatigue. Just after test, balls and plates appeared to be highly polished in wear tracks but became slightly tarnished approximately one week after test. Retainer insert wear was high and would be considered unacceptable for high speed ball bearings in an actual application.
2	440C	440C	Ag-MoS_2	2	Time = 10 hours	Wear of retainer inserts was higher than observed in Test No. 1. Balls and plates were again highly polished in the ball tracks just after test but became slightly tarnished after a period of time. Build-up of retainer material on balls and plates was greater than in Test No. 1 and is consistent with higher retainer wear.
3	440C	440C	Ag-MoS_2	4	Time = 10 hours	In spite of the unacceptable insert wear revealed in Tests No. 1 and 2 above, this candidate was subjected to tests at equivalent DN values of 4 x 10^6 to confirm the excellent lubricating characteristics at the higher speed. Condition of the balls and plates was essentially the same as observed in Test No. 2 (no evidence of fatigue). Insert wear was slightly higher than experienced in Test No. 2.

Table V-1 (Continued)

Test No.	Candidate Materials Balls	Plates	Inserts	Equivalent DN Value x 10^6	Hours To Failure	Remarks
4	440C	440C	$Ag-CaF_2$	2	Time = 2.5 hour	Plates were heavily coated with insert material. Balls were worn. Inspection showed ball diameters were .005 in. under the pre-test value. Balls also appeared to be dented as if the ball had encountered debris during operation. Retainer inserts were fractured in several pieces. Failure is attributed to the brittle fracture of the inserts rather than ball damage. The ball damage is believed to be a result of the poor insert performance.
5	440C	440C	$Ag-CaF_2$	2	Time = 3.5 hours	Results were same as those reported in Test No. 4 above using the same candidate material at the same test condition. Ball diameters were reduced by a full .001 in.
6	440C	440C	Salox M	2	Time = 10 hours	Balls and plates in excellent condition and retainer insert wear was low and certainly comparable to the wear rate observed in tests of the standard material Rulon A. Both balls and plates had faint bronze hue after testing.
7	440C	440C	Salox M	4	Time = 10 hours	In view of the excellent performance of this candidate in the above low speed test, a high speed test was immediately scheduled to follow. Performance was again excellent and insert wear was actually somewhat lower than seen in the low speed test. This occurence is discussed in the attached text.

Table V-1 (Continued)

Test No.	Candidate Materials Balls	Plates	Inserts	Equivalent DN Value x 10^6	Hours To Failure	Remarks
8	440C	440C	Salox M	4	Time = 10 hours	A second high speed test was scheduled to confirm the excellent performance and low insert wear of this candidate material at the high speed condition. This Performance was confirmed and the results compared closely with those of Test No. 7. At this time, this material candidate has shown performance superior to the Rulon A standard.
9	440C	440C	Boron Nitride	2	Time = .75 hours	Balls and plates were worn and pitted and generally speaking in worse condition than seen in any previous test. Ball diameters were reduced by .0025 in. Retainer insert wear was high. Performance of this candidate is considered poor.
10	440C	440C	Boron Nitride	2	Time = 5.5 hours	Low speed test rescheduled to confirm poor performance of this candidate in Test No. 9. Results of this test were worse than before and probably due to the higher test time accumulated before abort, which was erroneously set at a high level. Balls were reduced in diameter due to heavy wear. Diameter reduction was .012 in.
11	440C	440C	SP-3	2	Time = 10 hours	Balls and plates in good condition and no evidence of fatigue. Balls were heavily coated with insert material. Insert wear was moderate but would be considered high for an actual ball bearing application.

Table V-1 (Continued)

Test No.	Candidate Materials Balls	Plates	Inserts	Equivalent DN Value x 10^6	Hours To Failure	Remarks
12	440C	440C	SP-3	2	Time = 10 hours	Results same as in previous low speed Test No. 11.
13	440C	440C	SP-3	4	Time = 4.7 hours	Plates and balls damaged. Retainer insert wear was very high. Performance of this candidate considered inferior to Rulon A standard because of higher retainer insert wear.
14	440C	440C	Salox Z-1	2	Time = 10 hours	Balls and plates in good condition but insert wear was extremely high. In fact balls wore completely through the walls of the insert and started rubbing aluminum carrier plate.
15	440C	440C	Salox Z-1	2	Time = 10 hours	A second low speed test with this candidate was scheduled to confirm poor wear characteristics of this insert material observed in Test No. 14. Results of this test were far worse than in previous test due to an apparent failure of the abort system. Recording of the load arm accelerometer showed that the axial vibration increased after 5.5 hours of operation. This is believed to be the point where complete insert wear occurred and consequently where the test should have been aborted.
16	440C	440C Plated with MLF-5	Rulon A	2	Time = 10 hours	Balls and plates in good condition. Retainer insert wear was low as expected.
17	440C	440C Plated with MLF-5	Rulon A	2	Time = 10 hours	Same results as in Test No. 16.

Table V-1 (Continued)

Test No.	Balls	Plates	Inserts	Equivalent DN Value x 10^6	Hours To Failure	Remarks
22	440C	440C Plated with Fluorglide	Rulon A	4	Time = 4.5 hours	No preliminary test at low speed condition thought necessary since Rulon A inserts were used. The effect of plating the plates with a fluorocarbon coating could therefore be evaluated at high speed by comparing those results with performance of the standard. The results of this test showed the plates and balls to be damaged. It is thought the damage was due to the relatively thick (.001 in.) coating. The coating appeared to have been moved and collected thereby fouling the ball path and causing failure. Rulon A insert wear was high.
23	440C	440C Plated with Fluorglide	Rulon A	2 (see remarks)	Time = 5.75 hours (see remarks)	This was intended to be a second high speed test. Run was stopped when it was discovered that speed had been erroneously set. The resulting test conditions are: Hertz stress = 250,000 psi; spin roll ratio = .295; and ball rotational velocity = 109,000 rpm. Balls and plates in good condition. Insert wear was low.

The next series of tests was conducted with Salox M retainer inserts and unplated AISI 440C balls and plates, the only candidate material combination that exceeded the performance of the Rulon A standard. The first test was conducted at an equivalent DN level 2 x 10^6 and post-test inspection showed the balls and plates to be in excellent condition and having a slight bronze-colored hue. The retainer wear was extremely low as shown in figure V-3 and certainly no higher than observed in the Rulon A standard tests. In fact, the tests specimen were in such excellent condition that an immediate test was scheduled at the higher equivalent DN value of 4 x 10^6 mm-rpm. The candidate specimen successfully completed the 10-hour endurance run at high speed and the insert wear was found to be actually lower than had been found in the low DN test. A third high speed test was conducted to confirm the low wear and the results were identically reproduced. See figure V-3 for retainer wear resulting from this third test. The exact reason for the lower wear in the high DN tests is not known.

This series of tests with the Salox M candidate proved that this material is superior to Rulon A. Coincidentally, some recent tests with RL10 bearings using Salox M retainers have resulted in lives in excess of 60 hours at DN values of approximately 1 x 10^6 mm-rpm. For a cryogenic bearing and current rocket engine, this represents a significant increase in life over present standards.

Boron nitride, or white carbon, was used as the retainer inserts in the next series of tests. As shown in table V-1, the results of two low DN tests were poor and this candidate did not qualify for higher equivalent DN tests. Both balls and plates were badly worn and pitted and generally speaking in far worse condition than any specimens tested up to this time. Balls in both low speed tests were reduced in diameter by .0025 in to .012 in. The wear rate on the other hand was high but not excessive and is shown in figure V-4. It appeared that the insert had the capability of protecting itself even from the adverse ball surface but performed poorly as a lubricant for the ball-plate contact area. It should be pointed out that after the material was procured for testing, it was learned that it readily absorbs water vapor from the environmental surroundings. In a hydrogen compartment, this would present no problem, but the practical aspects of protecting the material in the manufacture, assembly, and shipment of engines would be severe. The decision was therefore made that no special protective procedures would be employed in these candidate tests in order that the simulation would be fair. Absorption of the water and subsequent freezing of same is thought to be responsible for the breakage of these specimens.

The next series of tests were conducted with SP-3 retainer inserts. SP-3 is a relatively stiff polymer (polyimide) filled with 15% by weight of MoS_2. From a life standpoint this candidate material, as shown by the results of table V-1, was comparable to the Rulon A standard material. On the other hand, the wear rate with SP-3 inserts was higher than experienced with the Rulon A inserts (see figure V-5). Again, however, the material appeared to have some promise as a candidate and the high speed test was conducted in spite of the high wear. In this test the specimen failed due to very high wear of retainer insert in 4.7 hours.

The results of the next series of tests with Salox Z-1 retainer inserts and AISI 440C balls and plates were suprisingly poor. It was thought that the combined lubricating characteristics of MoS_2 and the wear resistance of the fluorocarbon retainer insert matrix would provide almost ideal conditions. The balls and plates were in good condition but the retainer wear, as shown in figure V-6, was extremely high in the first low DN test. In the second low DN test, the abort system failed to function properly but a recording of the load arm accelerometer showed a drastic increase in vibration after 5.4 hours. This is thought to be the point where the ball wore completely through the insert and began to rub directly on the aluminum carrier. The test ordinarily would have been aborted at this point. However continuous operation under this adverse condition caused extreme damage to the balls and plates.

The results of the Al-MoS_2 retainer inserts with unplated AISI 440C balls and plates were poor. The balls and plates were in fair condition after 10 hours at the low DN test level but the retainer insert wear was high. See figure V-7.

The final series of tests in this program task were conducted with Rulon A retainer inserts, AISI 440C balls, and AISI 440C plates plated with MLF-5 dry film lubricants.

The performance of this candidate was excelled at both low and high equivalent DN values. In all cases the Rulon A insert wear was low and comparable to the wear observed in the standard tests. From a life standpoint, this candidate exceeded the performance demonstrated by the standard material combination. The wear tracks on the test plates were in excellent condition and had a slight golden hue. This coloring has been attributed to either the gold in the MLF-5 coating or the Rulon A which was transferred from the retainer to the plate by the ball.

Performance of this candidate is considered superior to the standard material combination.

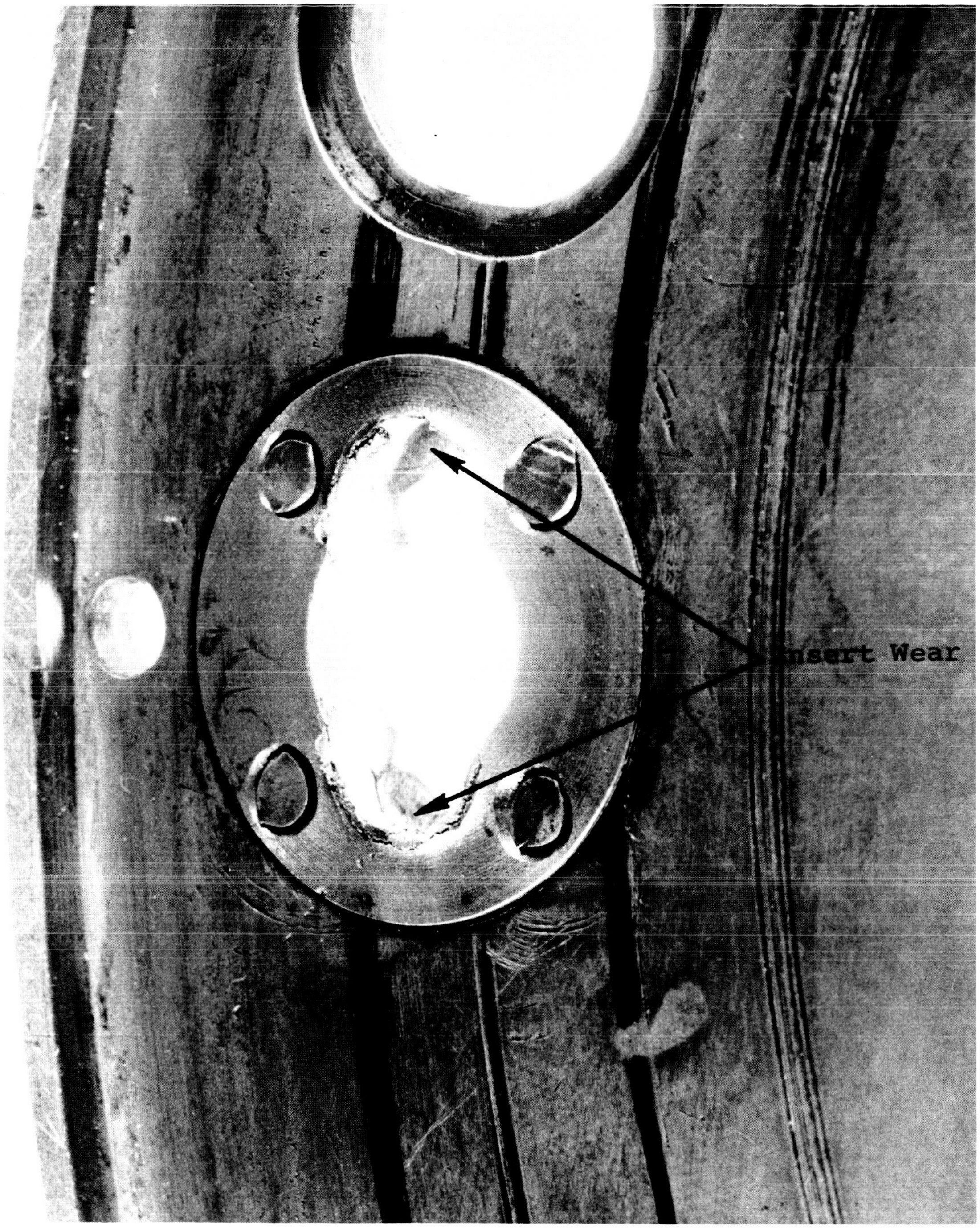

Figure V-1. Typical Retainer Insert Wear (Ag-M_oS_2 After 10 Hours at Equivalent DN Value of 4×10^6 mm-rpm) FE 41337

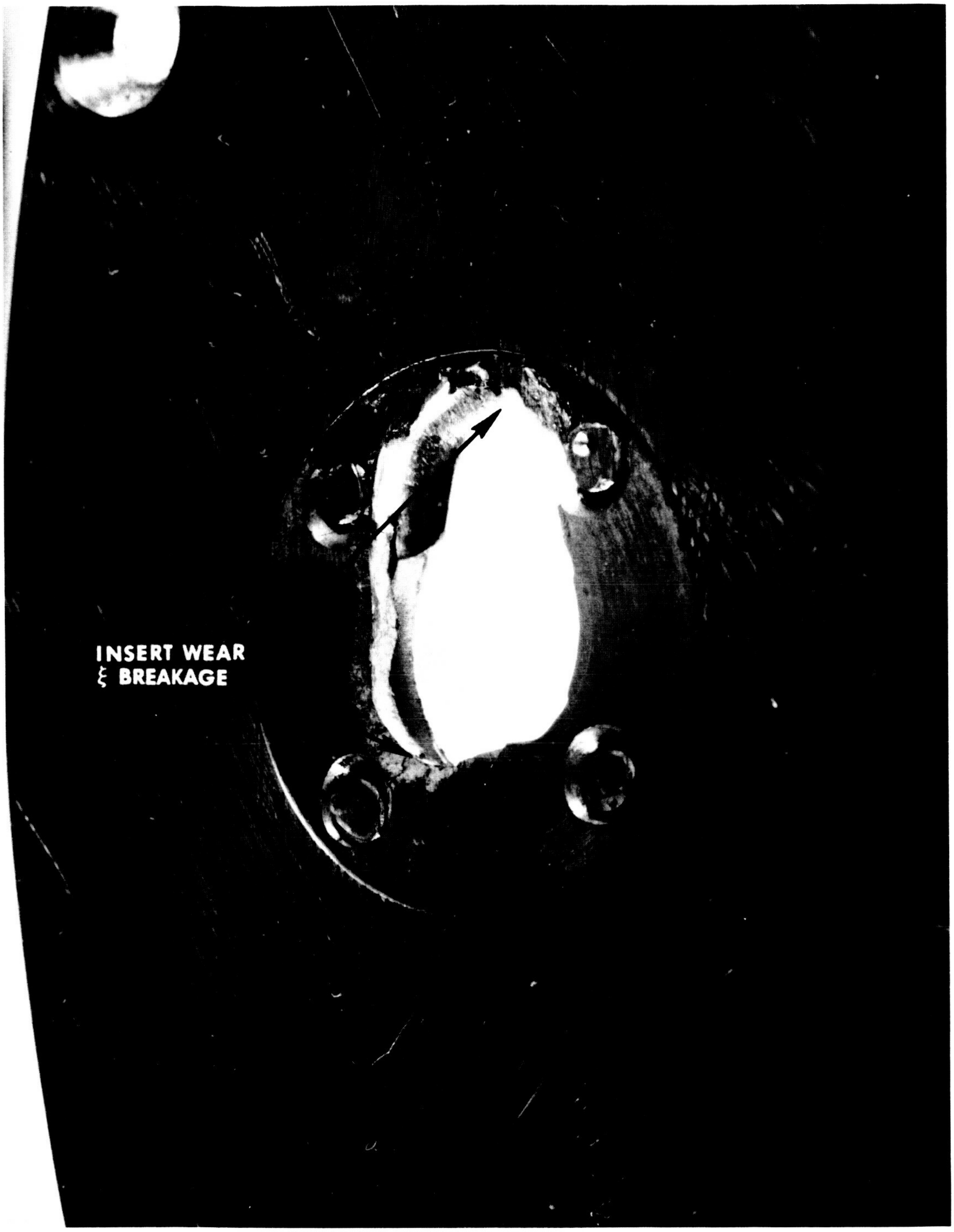

Figure V-2. Typical Retainer Insert Wear (Ag-CaF_2 After 3.5 Hours at Equivalent DN of 2×10^6 mm-rpm) FE 41333

FE 42225

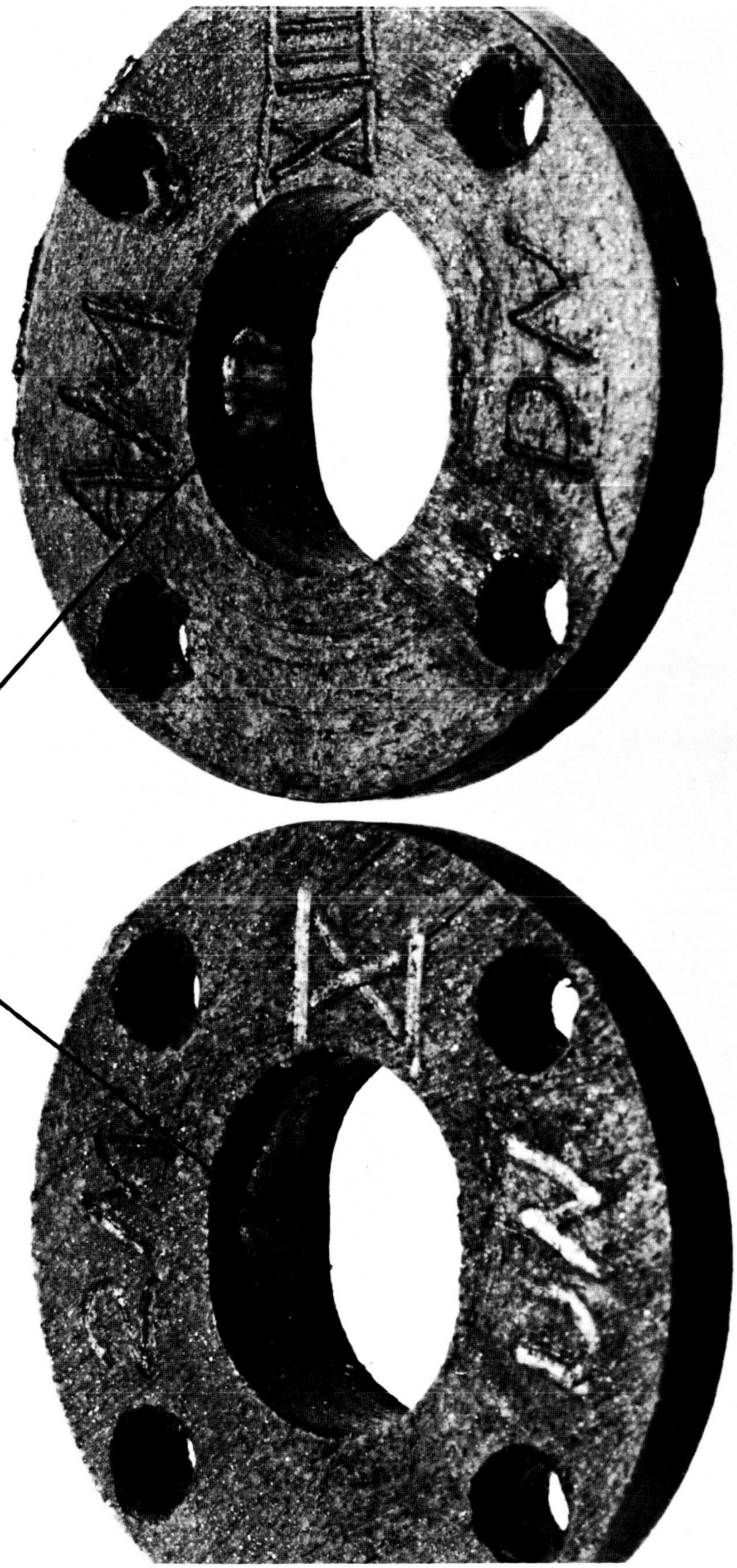

Figure V-3. Salox M Insert Wear

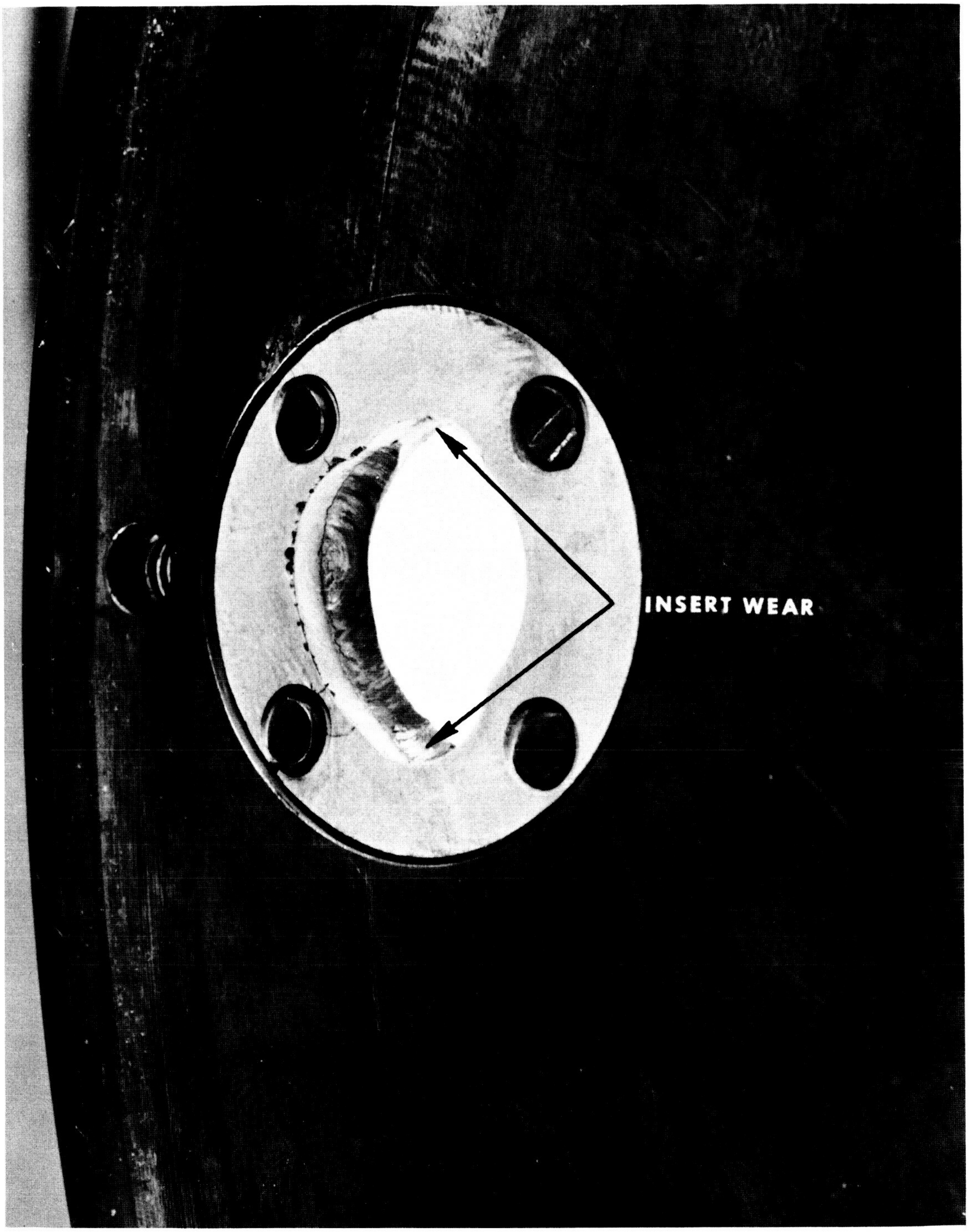

Figure V-4. Typical Retainer Insert Wear (BN After 5.5 Hours at Equivalent DN Value of 2×10^6 mm-rpm) FE 41335

Figure V-5. Typical Retainer Insert Wear (SP-3 After 10 Hours at Equivalent DN Value of 2×10^6 mm-rpm) FE 41334

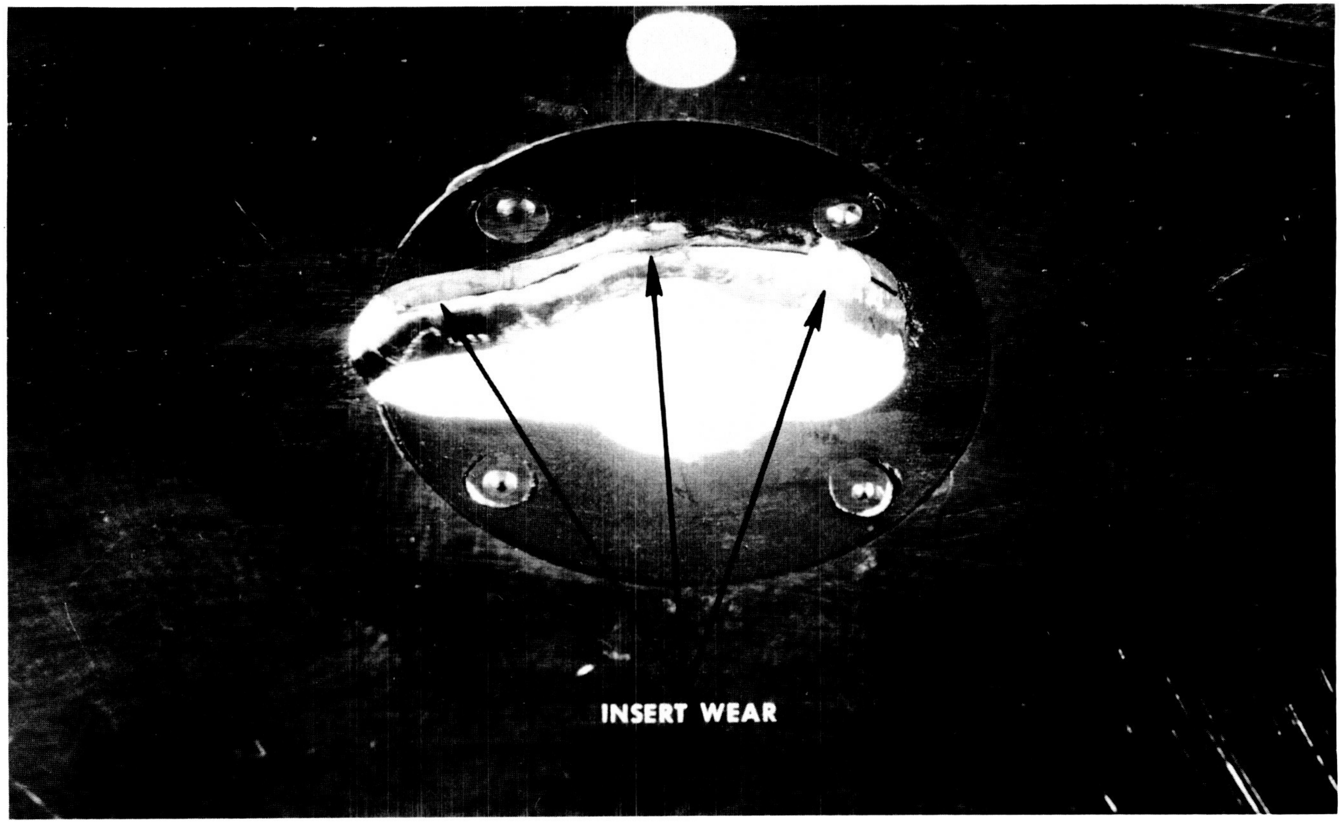

Figure V-6. Typical Retainer Insert Wear (Salox Z-1 After 10 Hours at Equivalent DN Value of 2×10^6 mm-rpm) FE 41332

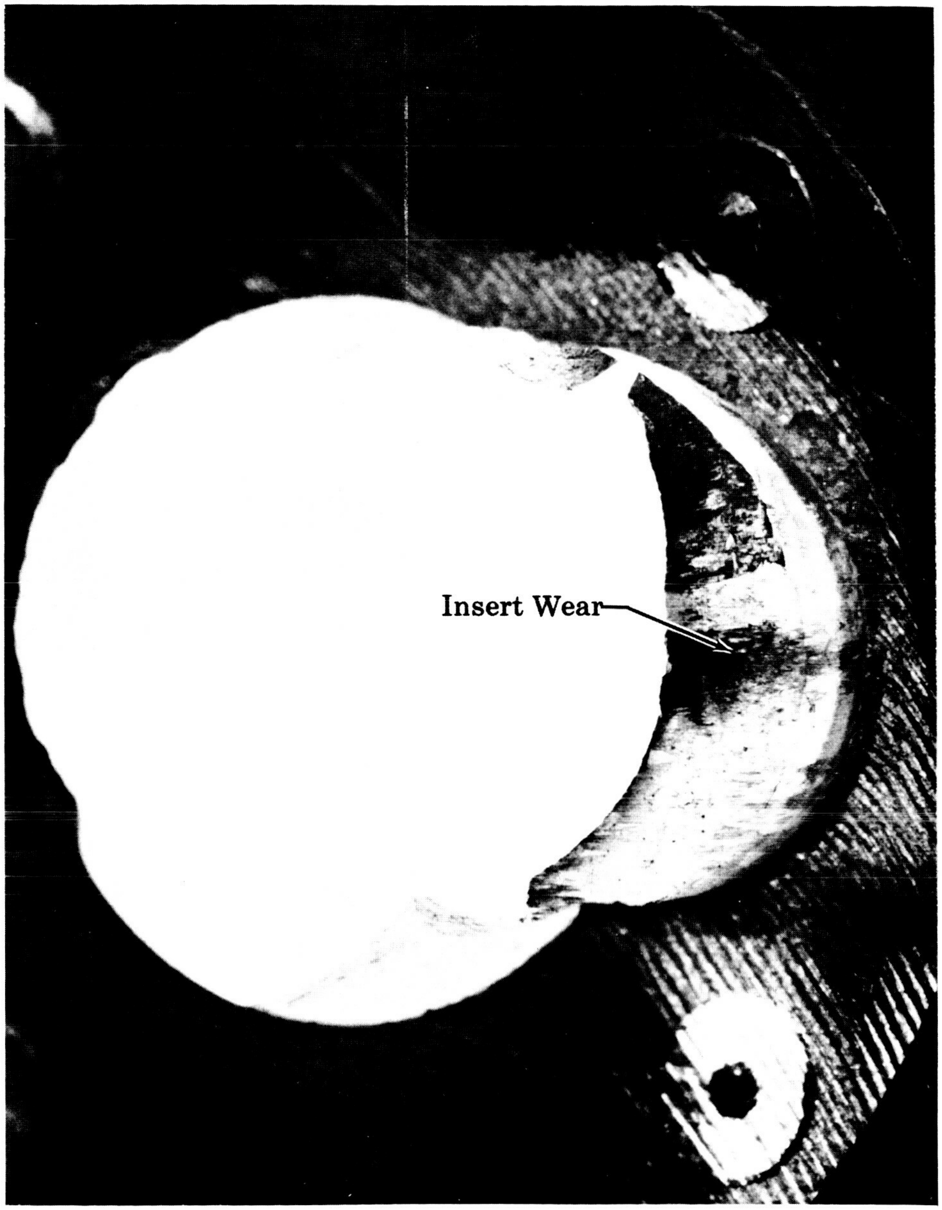

Figure V-7. Al-MoS_2 Insert After 10 Hours Operation at DN = 2 x 10^6 mm-rpm FD 8192

SECTION VI
CONCLUSIONS

The results of this program have shown that for rolling element bearings operating in liquid hydrogen at DN values up to 4 x 10^6 mm-rpm under Hertz stress levels up to 250,000 psi and spin/roll ratios up to .30, the most efficient material combinations explored in this investigation can be listed as follows in order of decreasing level of overall performance.

Rank	Retainer Material	Ball Material	Race Material
1	Salox M	AISI 440C	AISI 440C
2	Rulon A	AISI 440C	AISI 440C + MLF-5 coating
3	Rulon A	AISI 440C	AISI 440C

The first two material combinations demonstrated lives in excess of 10 hours and extremely low retainer wear rates while operating under all test conditions. The third combination, which was used as the standard in this experimental program, demonstrated a life in excess of 10 hours at a DN value of 2 x 10^6 mm-rpm and approximately five hours at DN value of 4 x 10^6 mm-rpm. The wear rate in both cases was low.

Since all of the above material combinations utilize retainers made of a composite containing polytetrafluroethylene, none can be considered satisfactory for applications where nuclear environments exceed 10^5 ergs per gram (c). This is generally accepted as the critical dosage beyond which the organic compound loses its strength.

All candidate material combinations that are compatible with hotter nuclear environmental failed to meet the performance requirements established by the standard materials. However, two of these combinations (one using SP-3 retainer inserts and the other using Ag-MoS_2 retainer inserts) did show sufficient promise to warrant further investigation.

For instance, the material combination using SP-3 retainers demonstrated excellent life at a DN value of 2×10^6 mm-rpm and approximately five hours at a DN value of 4×10^6 mm-rpm. But the wear in all instances was high, especially in the higher speed tests. The high wear is thought to be a result of the relatively low thermal conductivity of the polyimide matrix. The retainer material could not rid itself of the heat generated by the rotating ball and high wear resulted. It would appear that addition of materials such as silver or copper in the SP-3 composite might eliminate or at least alleviate this problem. The critical nuclear radiation dosage of this material is reported to be 7×10^7 ergs per gram (c).

Another material combination using Ag-MoS_2 retainer and AISI 440C balls and races demonstrated lives in excess of 10 hours at both DN levels of 2×10^6 and 4×10^6 mm-rpm. But the retainer wear was very high. This combination would have no trouble in nuclear environments up to 10^{15} ergs per gram (c) and for this reason any effort to solve the high wear problem would seem worthwhile. It does not have the thermal conductivity difficulties of the SP-3 candidates, and the high wear is thought to be a result of its low hardness and moderate modulus of elasticity. Various materials could be used to improve these properties and consequently its wear resistance without greatly harming its excellent lubricating characteristics.

As a third conclusion, it can be stated that under the levels of combined rolling and slip used in this program, boran nitride and calcium fluoride cannot be considered as lubricants in a liquid hydrogen environment. Various degrees of ball wear occurred in each of the tests conducted with candidates using retainers containing these materials.

SECTION VII
REFERENCES

1. Jaffe, L. D., J. B. Rittenhouse, "Behaviour of Materials in Space Environments," ARS Journal, March 1962.

2. Orcutt, F. K., H. H. Krause, C. M. Allen, "The Use of Free-Energy Relationships in The Selection of Lubricants for High-Temperature Applications," Wear, 5, 1962.

3. "Breaking Lubrication Barriers," Bulletin 121, Alpha-Molykote Corp., Stamford, Conn.

4. Peterson, M. B., R. L. Johnson, "PbO and Other Metal Oxides as Solid Lubricants for Temperatures to 1000°F," ASLE/ASME Preprint No. 56 LC-10, October 1956.

5. Johnson, R. L., H. E. Sliney, "Ceramic Surface Films for Lubrication at Temperatures to 2000°F," Ceramic Bulletin Vol. 41, No. 8, 1962.

6. Campbell, M. E., J. W. VanWyck, "Development of Design Criteria for a Dry Film Lubricated Bearing System," ASD-TDR-62-1057, March 1963.

7. Devine, M. J., E. R. Lawson, J. H. Bower Jr., "Anti-Friction Bearing Design Considerations for Solid Lubrication," ASME Preprint 63-MD-43, May 1963.

8. "Survey of Materials for High-Temperature Bearing and Sliding Applications," DMIC Memo No. 106, Battelle Memorial Institute, 12 May 1961.

9. Stocker, W. M. Jr., "Breakthrough in Dry Lubrication," American Machinist/ Metalworking Manufacturing, 11 June 1962.

10. Matt, R. J., J. B. Muratone, R. E. Murteza, C. J. Zupkus, "Research and Development of Airframe Bearings for Aerospace Vehicles, Progress Report No. 1, 2, 3, and 4, Contract AF33(657)-8431, 1 August 1962, 8 November 1962, 11 February 1963, and 7 May 1963, respectively.

11. Brown, R. D., R. A. Burton, P. M. Ku, "Friction and Wear Characteristics of Cermets at High Temperature and High Vacuum," ASD-TR-61-301, September 1961.

12. Moon, D. P., J. A. Van Echo, W. F. Simmons, J. F. Barker, "Structural Damages in Thermally Cycled Rene 41 and Astraloy Sheet Materials," OTS PB 151083, DMIC Report No. 126, Battelle Memorial Institute, Defense Metals Information Center, 29 February 1960.

13. Brown, R. D., R. A. Burton, P. M. Ku, "Research on High Temperature Bearings," ASD-TR-61-705, August 1962.

14. Daniel, B., "Solid Film Lubricants for High Temperature Nuclear Environments," WADD Technical Report 60-823, Part II, September 1961.

15. Lavik, M. T., "High Temperature Solid Dry Film Lubricants," Midwest Research Institute, October 1958, WADC-TR-57-455 Part II ASTIA Doc. No. 203121, Wright Air Dev. Center.

16. Diennes, G. J., and G. H. Vineyard, "Radiation Effects in Solids," Interscience Publishers, Inc., Vol. II, New York 1957.

17. Ellis, R. H., "Nuclear Technology for Engineers," McGraw-Hill Book Co. Inc. 1959.

18. Glasstone, S., "Principles of Nuclear Reactor Engineering," D. Van Nostrand Co., Inc. 1961.

19. "Radiation Effects State of the Art," 1960-1961, Radiation Effects Information Center, Battelle Memorial Institute, Columbus 2, Ohio REIC Report No. 22, 30 July 1960.

20. "Radiation Effects on Reactor Metals," David O. Leeser, Nucleonics, pp 68, September 1960.

21. "Radiation from Nuclear Space Powerplants and Its Effect Upon Materials," Michael E. Ihnat, Avco. Res. & Adv. Dev. Div. AD 249502.

22. "Symposium on Radiation Effects on Materials," ASTM special Technical Publication No. 220, Vol. I and II, American Society for Testing Materials, 1961 Race St., Philadelphia 3, Pa.

23. Mehan, R. L., "Irradiation of Haynes - 25 and Inconel - X Compression Springs in High-Temperature High-Pressure Water," Journal of Basic Engineering, June 1959.

24. Billington, D. S., "Relaxing Reliance on Empirical Data," Nucleonics, September 1960.

25. Brace, D., "Solid Film Lubricants for High Temperature Nuclear Environments," Midwest Research Institute, September 1961, WADD TR 60-823 Part II, USAF Aeronautic Systems Division.

26. "Summation Report for Capsule PW 24-1," from A. C. Loethen, D. R. Formelo, H. W. Ferry to R. V. Steel, (CANEL Rept.) Static Inpile Exam Results, FXM 6028, 6 December 1961, Contract AT(30-1)-2789.

27. Campbell, M. E., J. W. Van Wyck, "Development of Design Criteria for a Dry Film Lubricated Bearing System," ASD-TDR-62-1057, March 1963.

28. Devine, M. J., E. R. Lawson, J. H. Bower, "The Lubrication of Ball Bearings with Solid Films," ASME Preprint No. 61-LUBS-11, March 1961.

29. Lavik, M. T., T. M. Medued, and W. L. Clow, "Development and Evaluation of High Temperature Solid Film Lubricants," Progress Report No. 6, Contract No. AF33(616)-6854, Phase II, 30 September 1962.

30. Lewis, P., S. F. Murray, and M. B. Peterson, "Investigation of Complex Bearing and/or Lubrication Systems," MTI-62TR14, MTI-62TR34 & MTI-63TR5; First, Second, and Third Quarterly Progress Reports; 5 August 1962, 6 November 1962, and 12 February 1963, respectively, Contract AF33(657)-8666.

31. Macks, E. F., Z. N. Nemeth, and W. J. Anderson, "Preliminary Investigation of Molybdenum Disulfide - Air Mist Lubrication for Roller Bearings Operating to DN Values of 1 x 10^6 and Ball Bearings Operating to Temperatures of 1000°F," NACA RM E51G31, 1951.

32. Devine, M. J., E. R. Lawson, and J. H. Bower Jr., "Anti-Friction Bearing Design Considerations for Solid Lubrication," ASME Preprint 63-MD-43, May 1963.

33. Smith, L. L., "Fibrous Composite Materials for Extreme Environment Seals," ASLE Preprint 63AM-5B-2, April 1963.

34. "Advanced Data Sheet," Ilikon Corporation, Self Lubricating Materials.

35. Carrol, J. G., and R. O. Bolt, "Radiation Effects on Organic Materials," Nucleonics, pp 78, September 1960.

36. Seitz, Frederick, "The Effects of Irradiation on Metals," Rev. of Modern Physics, Vol. 34, No. 4, October 1962.

37. Jaffe, L. D., and J. B. Rittenhouse, "Behavior of Materials in Space Environments," ARS Journal, Vol. 32, No. 3, March 1962.

38. Calkins, V. P., and C. G. Collins, "General Radiation Damage Problems for Lubricant and Bearing-Type Materials," ASLE Preprint No. 56 LC-2.

39. Harwood, J. J., H. H. Hausner, J. G. Morse, and W. G. Rauch, "Effects of Radiation on Materials," Reinhold Publishing Corp., New York, 1958.

40. "A Survey of Radiation Effects in Metals," AERE Technical Note by J. W. Glen, Gt. Br. AERE, Harwell, Berks, 1954.

41. "Disordering of Solids by Neutron Radiation," W. S. Snyder and J. Neufeld, Physical Review, Vol. 97, No. 6, 15 March 1955.

42. Brinkman, J. A., "On the Nature of Radiation Damage in Metals," Journal of Applied Physics, Vol. 25, No. 8, August 1954.

43. Snyder, W. S., and Jacob Neufeld, "Vacancies and Displacements in a Solid Resulting from Heavy Corpuscular Radiation," Physical Review, Vol, 103, No. 4, 15 August 1956.

44. Billington, D. S., "Ionizing Radiation and Metals," Scientific America, Vol. 201, No. 3, September 1959.

45. Lavik, M. T., "High Temperature Solid Dry Film Lubricants," WADC Technical Report 57-455, Part II, October 1958.

46. Johnson, V. R., and G. W. Vaughn, "Investigation of the Mechanism of MoS_2 Lubrication in Vacuum," Journal Applied Physics, Vol. 27, No. 10, October 1956.

47. Lavik, M. T., "Ceramic Bonded Solid-Film Lubricants," WADD Tech. Rep. 60-530, Part II, April 1961.

48. Johnson, R. L., and H. E. Sliney, "Ceramic Surface Films for Lubrication at Temperatures to 2000°F," Ceramic Bulletin, Vol 41, No. 8, 1962.

49. Buckley, D. H., M. Swickert, R. L. Johnson, "Friction, Wear, and Evaporation Rates of Various Materials in Vacuum to 10^{-7} mm Hg.," ASME/ASLE Preprint.

50. Lavik, T. M., T. M. Medued, and W. L. Clow, "Development and Evaluation of High Temperature Solid Film Lubricants," Quarterly Progress Report No. 6, July - 30 September 1962, Midwest Research Institute.

51. "New Dry Lubricant Survives Space Tests," Steel, 3 June 1963.

52. Perterson, M. B., and R. L. Johnson, "PbO and Other Metal Oxides as Solid Lubricants for Temperatures to 1000°F," ASLE/ASME Preprint No. 56 LC-10, October 1956.

53. Sliney, H. E., "Lubricating Properties of Lead-Monoxide-Base Coatings of Various Compositions at Temperatures to 1250°F," NASA memo 2 March 1959E, February 1959.

54. Bonis, L. J., and B. Manning, "Some Principles of Self-Lubricating Solid Materials for Outer Space Application," Ilikon Corporation, Natick, Mass., 3 May 1963.

55. Boes, D. J., "Long Term Operation and Practical Limitations of Dry, Self-Lubricated Bearings from 1×10^{-5} TORR to Atmospheric Lubrication," Engineering, April 1963.

56. "Completely Dry Lube for Space Environments," Space/Aeronautics, July 1963.

57. Palmer, E. B., "Four Types of Dry Film Lubricants," Materials in Design Engineering, August 1961.

58. Anderson, W. J., L. B. Sibley, and E. V. Zaretsky, "The Role of Elastohydrodynamic Lubrication in Rolling-Contact Fatigue," ASME, Journal of Basic Engineering, September 1963.